PERFORMANCE OF SPACE TIME BLOCK CODED BIT INTERLEAVED CODED MODULATION SYSTEMS FOR MOBILE COMMUNICATION CHANNELS

OMAR KHAZA'AL ISMAEIL

September 2014

PERFORMANCE OF SPACE TIME BLOCK CODED BIT INTERLEAVED CODED MODULATION SYSTEMS FOR MOBILE COMMUNICATION CHANNELS

A THESIS SUBMITTED TO
THE GRADUATE SCHOOL OF NATURAL AND APPLIED SCIENCES OF
ÇANKAYA UNIVERSITY

BY
OMAR KHAZA'AL ISMAEIL

IN PARTIAL FULFILMENT OF THE REQUIREMENTS FOR THE DEGREE OF
MASTER OF SCIENCE
IN
THE DEPARTMENT OF
ELECTRONIC AND COMMUNICATION ENGINEERING

September 2014

Title of the Thesis: **Performance of Space Time Block Coded Bit Interleaved Coded Modulation Systems for Mobile Communication Channels**

Submitted by **Omar Khaza'al ISMAEIL**

Approval of the Graduate School of Natural and Applied Sciences, Çankaya University.

Prof. Dr. Taner ALTUNOK
Director

I certify that this thesis satisfies all the requirement as a thesis for the degree of Master of Science.

Prof. Dr. Celal Zaim ÇİL
Head of Department

This is to certify that we have read this thesis and that in our opinion it is fully adequate, in scope and quality, as a thesis for the degree of Master of Science.

Assoc. Prof. Dr. Orhan GAZİ
Supervisor

Examination Date: 10.09.2014

Examining Committee Members

Assoc. Prof. Dr. Orhan GAZİ	(Çankaya Univ.)	
Assoc. Prof. Dr. Fahd JARAD	(THK Univ.)	
Assist. Prof. Dr. Behçet Uğur TÖREYİN	(Çankaya Univ.)	

STATEMENT OF NON-PLAGIARISM PAGE

I hereby declare that all information in this document has been obtained and presented in accordance with academic rules and ethical conduct. I also declare that, as required by these rules and conduct, I have fully cited and referenced all material and results that are not original to this work.

Name, Last Name : Omar Khaza’al ISMAEIL

Signature : 

Date : 10.09.2014

ABSTRACT

PERFORMANCE OF SPACE TIME BLOCK CODED BIT INTERLEAVED CODED MODULATION SYSTEMS FOR MOBILE COMMUNICATION CHANNELS

ISMAEIL, Omar Khaza'al
M.Sc., Department of Electronic and Communication Engineering
Supervisor: Assoc. Prof. Dr. Orhan GAZİ

September 2014, 61 pages

In this thesis concatenated systems involving bit interleaved coded modulation (BICM) and space time codes (STC) are inspected in detail. Space time block codes (STBCs) are used while forming the joint structures. Performance of the joint structures involving BICM and STCs for additive white Gaussian and mobile fading channels are measured via computer simulations. Iterative decoding logic is applied for the decoding of these joint structures. An alternative feedback path for the iterative decoding of BICM-STBC joint structures is proposed and simulation results showed that the proposed path result in better bit error rate performance. Concatenated BICM-STBCs are also used in cooperative communication structures. A signal combination method based on the linear combination of the signal probabilities coming from the relays is proposed and it is seen that proper choosing of the coefficients for the linear combination of the probabilities is an important criteria for the performance of the cooperated systems.

Keywords: Bit Interleaved Coded Modulation, Space Time Codes, Concatenated Structures, Iterative Decoding, Cooperative Communications.

ÖZ

UZAY ZAMAN KODLAMALI VE BİT SERPİŞTİRİLMİŞ KODLAMALI MODÜLASYON İÇEREN İLETİŞİM SİSTEMLERİNİN GEZGİN İLETİŞİM KANALLARI İÇİN BAŞARIMLARI

ISMAEIL, Omar Khaza’al
Yüksek Lisans, Elektronik ve Haberleşme Mühendisliği Anabilim Dalı
Tez Yöneticisi: Doç Dr. Orhan GAZİ
Eylül 2014, 61 sayfa

Bu tezde bit serpiştirilmiş kodlanmalı (BICM) sistemlerle uzay zaman kodlamalı (STC) sistemlerin birleşik yapıları ele alınmış ve detaylı olarak incelenmiştir. Uzay zaman kodu olarak blok uzay zaman kodları kullanılmıştır. Oluşturulan birleşik yapıların başarım grafikleri beyaz gürültülü ve mobil sönmeli iletişim kanalları için bilgisayar benzetimi yardımı ile ölçülmüştür. Birleşik yapıların çözümleri esnasında yinelemeli çözüm metodu kullanılmıştır. BICM-STBC birleşik yapısının yinelemli çözümü için alternatif bir geri besleme yöntemi önerilmiş ve bilgisayar benzetimleri sonucunda önerilen yöntemin literatürde kullanılan klasik yönteme göre daha iyi performans sergilediği görülmüştür. Önerilen birleşik sistemler işbirlikli iletişim sistemelerinde uyarlanmıştır. İşbirlikli sistemlerde, son alıcıda, rölelerden gelen sinyallerin olasılıklarının doğrusal olarak birleştirildiği bir yöntem önerilmiş ve sistemin performansının doğrusal birleşim esnasında seçilen katsayılara çok fazla bağlı olduğu görülmüştür.

Anahtar Kelimeler: Serpiştirilmiş Kodlanmış Sistemler, Uzay Zaman Kodlama, Birleşik Yapılar, İşbirlikli Sistemler, Yinelemeli Çözüm.

ACKNOWLEDGEMENTS

I would like to express my sincere gratitude to Assoc. Prof. Dr. Orhan GAZİ for this supervision, special guidance, suggestions, and encouragement through the development of this thesis.

It is a pleasure to express my special thanks to my family for their valuable support.

TABLE OF CONTENTS

Page

CHAPTERS

LIST OF FIGURES

FIGURES **Page**

LIST OF TABLES

LIST OF ABBREVIATIONS

BICM-ID	Bit Interleaved Coded Modulation with Iterative Decoding
MIMO	Multiple-Input and Multiple-Output
STTC	Space-Time Trellis Codes
STBC	Space-Time Block Codes
TCM	Trellis Coded Modulation
CSI	Channel Side Information
BI-STC-ID	BICM-ID Scheme Concatenate with STBC Scheme with Iterative Decoding
FED	Free Euclidean Distance
NRSC	Non-Recursive Systematic Convolution
SP	Set Partitioning Labeling
SISO	Soft-Input/Soft-Output
APP	A-Posteriori Probability
MAP	Maximum a-Posteriori Probability
MRC	Maximum Ratio Combining
MLD	Maximum Likelihood Detector
AWGN	Additive White Gaussian Noise
CIR	Channel Impulse Response
DF	Decode-And-Forward
AF	Amplify-And-Forward
BI-STC-ID-DF	Cooperative BICM-ID Scheme Concatenated with STBC with Iterative Decoding and with Decode and Forward

CHAPTER 1

INTRODUCTION

1.1 Background

The wireless communication systems are becoming an important and necessary part of our life in every day, for example, GSM, WLAN, internet applications, etc. Although the next-generations of mobile systems such as 3GPP (LTE) and fourth generation (4G) are able to support the different needs of users on different communication environments (mobile/cellular, office, home, etc.) [1], there is still a tendency to increase the data rate to deal with the growing demand for multimedia services such as network game, video teleconferencing, etc.

The technical challenge in the design of communication systems is to increase transmission data rate with an efficient bandwidth and an efficient power. The efficiency of the bandwidth means the minimum channel bandwidth needed for data transmission at the required data rate [2]. The minimum value of SNR (signal to noise power ratio) needed to get the required quality of service is defined as the power efficiency.

In mobile communication systems, the propagation path of radio signal from the transmitter to the receiver consists of multipath. The radio signal suffers from high noise and fading gain due to energy absorption by objects along the propagation paths and due to rapid fluctuations of the signal caused by the motions of receiver [3]. Fading gain is a random variable with distribution. One such distribution is the Rayleigh distribution which its real and imaginary parts are zero mean Gaussian random distributed.

A predominant way of adapting with the randomness of the fading channel is to use more than one antenna either at the transmitter or receiver or both, called MIMO systems (multiple-inputs and multiple-outputs systems). A MIMO system increases the diversity gain (spatial and coding diversity) by transmitting multiple copies of each symbol by multiple antennas over independent fading channels [4, 5]. The coding diversity means increasing the transmission reliability by transmitting multiple copies of each symbol. The spatial diversity means increasing the transmission data rate (capacity).

Transmitting multiple copies of each symbol results in the symbol rate of the MIMO system seems to decrease, but leads to increase the diversity of the system. The MIMO system increases the probability of arriving one copy of the signal at least to the receiver with low fading. This increment can be maximized by multiplying the number of transmitter antennas with the number of receiver antennas [4]. The use of multiple antennas in communication systems is practically limited in the base stations because of leading to increase the complexity of mobile devices. MIMO schemes are considered to be the preferred candidate for the next-generation of mobile systems due to providing high data rate and high quality of services.

Two basic schemes of the space-time codes (STC) are space-time trellis codes "STTC" and space-time block codes "STBC" [4]. Both schemes can provide high spatial diversity. STBC is different from STTC in the sense that STBC provides coding gain less than STTC. STBC is considered more appropriate for practical systems because its complexity and its cost are less than STTC.

STBC scheme proposed by Alamouti [6] is a simple communication system employing two antennas at the transmitter and uses a simple decoding algorithm which can be generalized to any arbitrary number of antennas at the receiver.

In STBC communication systems, the transmitter diversity is achieved by transmitting two independent copies of the same symbol taking into consideration that if one of the copies is faded seriously the other copy is received with higher power [5].

STBC scheme does not provide coding gain, but only diversity gain. In order to get coding gain in addition to spatial gain, suitable coded modulation schemes can be concatenated with STBC to improve performance. In this approach STBC is concatenated with bit-interleaved coded modulation with iterative decoding (BICM-ID) proposed by Li and Ritcey which was studied in [6, 7].

In BICM-ID scheme, convolutional encoding is connected with the 8-PSK modulator process (Mapper) through S-random bit interleavers to improve the spectral efficiency of the wireless communication systems. This leads to increase Euclidean distance between symbol sequences and hence improve the performance of communication systems.

The use of S-random bit interleavers in BICM-ID scheme improves the performance of the system over Rayleigh slow fading channel by increasing the diversity gain. The S-random bit interleaver breaks the correlation that may occur between the transmitted bits. However, the S-random bit interleaver results in the decrement of the Euclidean distances which decreases the performance over AWGN channel. The iterative process in BICM-ID scheme is used to improve the performance of the system through decreasing the bit error rate at the receiver by repeating the decoding process several times.

The BI-STC-ID joint structure is preferred in mobile communication systems because it provides high data rates on Rayleigh slow fading channel [8]. The transmitter of BI-STC-ID joint structure consist of a concatenated structure involving an outer convolutional encoder, bit interleaver, 8-PSK modulator, symbol interleaver and an inner STBC encoder. At the receiver side to extract the transmitted data information from the received signal, the receiver structure consists of an inner decoder, symbol de-interleaver, demodulator, bit de-interleaver and an outer decoder which function iteratively [8].

The joint structure involving STBC and BICM provides spatial diversity and coding gain through using multiple antennas at the transmitter and receiver sides. This leads to an increment in the area covered and the data rate without increasing the bandwidth and the transmitted power. The small size of the receiver mobile unit limits the number of antennas because of the power consumption and the complexity. A cooperative diversity suggested by Nosratinia is applied on BI-STC-ID scheme to get enormous potential for the next generations of wireless communication networks. In cooperative systems several intermediate stations named as relays are distributed between the source and the destination in different paths. The cooperative communications make the whole system more reliable with respect to the amount of throughput and the term of bit error rate (BER).

1.2 Objectives

In this thesis, the main aim of this study is to improve the performance of the wireless systems without increasing the transmitted power and the data rate by using the coding techniques. We studied the performance of BICM-ID communication system over AWGN and mobile fading channels. We simulated this communication system by C++ programming and we got the simulation results as a BER vs. $E_b/N_\circ$ curve. A comparison between the performance of this system and the performance of the conventional BICM schemes is conducted. We tried to improve the performance of communication systems by merging the performance of two schemes together involving a BICM-ID scheme and STBC to form BI-STC-ID joint structure with iteration process. Next curve. We improved the performance of the joint structure scheme more by executing the iteration process between the outer convolutional decoder and the inner STBC decoder rather than being between the outer convolutional decoder and the demodulator. This modification in feedback connection leads to decrease the BER curve as we will see in Chapter-5. The Cooperative communication systems were studied which involves the joint structure BI-STC-ID scheme. The Cooperative diversity converts the single source and single destination communication structures to structures consist from multiple sources and multiple destinations by adding cooperative secondary stations with a DF protocol between the transmitter and the receiver. This cooperative system has been simulated and the simulation results have been sketched as a BER vs. $E_b/N_\circ$ curve.

1.3 Organization of the Thesis

The outline of this thesis is as follows, Chapter-1 is an introduction and literature review for the main and secondary communication schemes used in this thesis like cooperative BI-STC-ID scheme in addition to review the purpose of this thesis. Chapter-2 contains the description of the transmitter and receiver modules for BICM-ID scheme to review the parameters of the system's design in detail. The methods of labeling process on the transmitter module are described to illustrate its importance on optimizing the different methods of decoding at the receiver module. The rules of

designing S-random interleavers are also reviewed. In addition the computations of bit metrics, branch metrics and feedback metrics at the receiver model are reviewed.
Chapter-3 describes the encoding and decoding processes for STBC in detail and reviews its importance to improve the wireless systems by increasing the spatial diversity and coding gain. This chapter also reviews the process of connecting the coded modulation BICM-ID scheme with the STBC to form BI-STC scheme and illustrates its importance to improve the wireless systems by increasing the data rate and the reliability of the received data. In addition, this chapter describes the wireless channel models used in this thesis and computes their parameters.

In Chapter-4 the cooperative communication systems have been studied to illustrate its improvement in the performance. The cooperative BI-STC scheme has been described and formed by using secondary stations (relays) between the transmitter and the receiver. Several types of signal combination techniques are reviewed in this chapter to combine the received signals from the source and relay nodes at different time slots.

Chapter-5 contains the simulation results of BICM-ID, BI-STC-ID and cooperative BI-STC-ID schemes over AWGN and Mobile fading channels as BER vs. $E_b/N_\circ$ curves. This chapter also reviews a comparison between the performances of these wireless schemes by observing their simulation results.

Finally, Chapter-6 contains the conclusions from simulating the different communication schemes after observing the simulation results, also this chapter contains the future works which we got them according to the simulation results.

CHAPTER 2

BIT INTERLEAVED CODED MODULATION WITH ITERATIVE DECODING (BICM-ID)

2.1 Introduction

The frequency spectrum of the radio signals is considered as a rare resource. Thus, one the most important goal in the design of digital wireless communication systems is to exploit the available spectrum efficiently to meet the demands of growing traffic with time. In 1982, Ungerboeck proposed a Trellis-Coded Modulation (TCM) scheme for AWGN channels to increase the efficiency of frequency spectrum in communication systems which was developed for mobile communications later. TCM scheme improves the spectrum efficiency by merging the coding and modulation processes which lead to the large Euclidean distances between the symbols [9].

In practical wireless systems such as mobile radio and indoor wireless systems, the radio signals propagate from the transmitter to the receiver in a multipath environment. The communication channel in these systems can be represented as a Rayleigh fading channel. TCM scheme usually has low performance on a fading channel because it has low diversity [9]. The performance of coded scheme in communication systems over fading channels depends on a code diversity strongly. In order to improve the performance of TCM over Rayleigh fading channels, bit interleaved coded modulation (BICM) scheme proposed by Zehavi is considered one of many adaptations for the improvement [10].

BICM scheme provides high improvement by increasing diversity gain through using bit interleaver in conjunction with Gray labeling instead of symbol interleaver in traditional TCM. The use of bit interleaver leads to increase the reliability of the coded system on fading channels, but also leads to deterioration in the performance on AWGN channels. This deterioration occurs due to the reduction in Euclidean distance between the coded symbols due to the random modulation caused by bit interleaver. In order to take full benefits of bit interleaver, an iterative process at the receiver is employed to improve the performance on the AWGN channel through reducing the bit error rate.

2.2 Principle of BICM

The structure of the transmitter module for BICM scheme is shown in Fig. 1. This structure consists of rate-2/3 non-recursive convolutional encoder, S-random bit-interleavers, and 8-PSK modulator (with Gray labeling), [11].

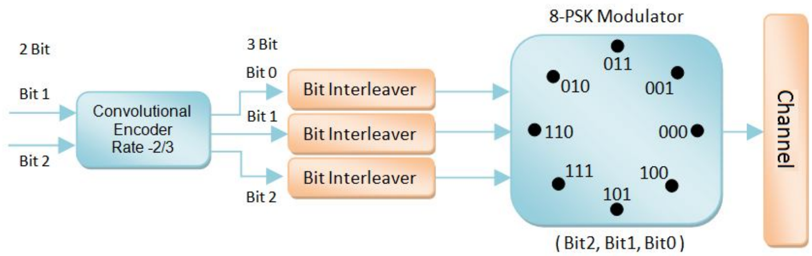

Figure 1 The structure of the transmitter module for BICM scheme

The purpose of S-random interleaver is to improve performance of the BICM scheme by dispersing the similarity between the transmitted bits on fading environment. The interleaved bits are grouped and converted to complex symbols using an 8-PSK modulator. The Gray labeling is used in the modulator to get optimal system performance [12].

The type of the convolutional encoder used in BICM scheme is Paaske's non-recursive convolutional encoder which was suggested in [13]. It provides larger Hamming distance to get optimal performance on fading channel. Paaske's non-recursive convolutional encoder of 8-state with rate-2/3 is shown in Fig. 2.

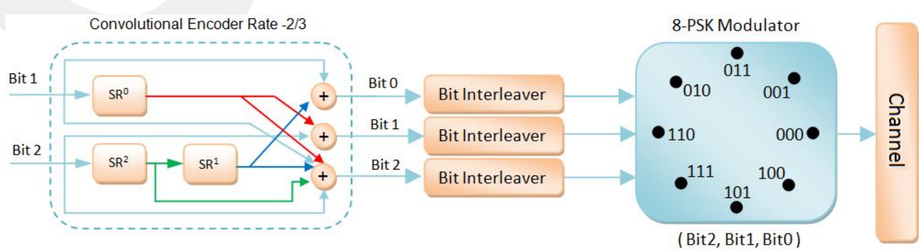

Figure 2 Paaske's non-recursive convolutional encoder with 8-state and rate-2/3

The structure of the receiver module for BICM scheme is shown in Fig. 3. The receiver implements similar processes as the transmitter does, but in an inverse manner. The inverse list of processes consists of the concatenation of the 8-PSK demodulator and convolutional decoder [14]. For each received symbol, the demodulator computes six values of bit metrics related to the three bits positions in each symbol.

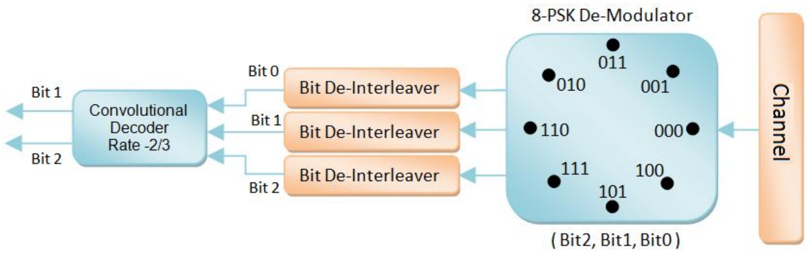

Figure 3 The structure of the receiver module for BICM scheme

The computed values of the bit-metrics at the output of demodulator are de-interleaved by using three S-random bit de-interleavers to estimate the original codewords. Then the estimated codewords are decoded by the convolutional decoder through generating the best suitable estimation of the information bits sequence [14].
BICM scheme shows low performance on AWGN channels comparing to TCM scheme due to the bit interleaver. The bit interleaver minimizes the free Euclidean distances between the coded symbols through randomizing the modulation process. The 3-bits assigned to each of 2^3 symbols are randomized by using three independent bit interleavers [16].
Paaske's non-recursive convolutional encoder has rate-k/n, where k is the number of information bits at the input of the encoder and n is the number of bits at the output of the encoder. Paaske's encoder has 2^h states, where h represents the constraint length of the convolutional encoder.
The convolutional encoder used in this thesis has 8 states. The impulse responses and the generator matrix in polynomial form are given as follows:

$$g_1 = [g^0 \ g^1 \ldots.. \ g^n] = [D^2 \quad D \quad D + D^2]$$
$$g_2 = [g^0 \ g^1 \ldots.. \ g^n] = [1 \quad D^2 \quad 1 + D + D^2]$$
$$G(D) = \begin{bmatrix} g_1 \\ g_2 \end{bmatrix} = \begin{bmatrix} 1 & D & 1 + D \\ D^2 & 1 & 1 + D + D^2 \end{bmatrix} \qquad (2.1)$$

where g_1, g_2 are the generator polynomials of convolutional encoder which can be represented in octal form as :

$$g_1 = [4\ 2\ 6] \quad g_2 = [1\ 4\ 7] \tag{2.2}$$

2.3 Example of Encoding Process in BICM

In order to illustrate the encoding process in BICM scheme, an example of Paaske's non-recursive convolutional encoder is shown in Fig. 4. It is obvious from the figure that the convolutional encoder has 2 inputs and 3 outputs with rate-2/3. Each 2-bit dataword of the information bits denoted by d= (d^1, d^0) are encoded to generate 3-bit codeword denoted by c= (c^2, c^1, c^0). The convolutional encoder consists of 3 memory cells denoted by (SR^2, SR^1, SR^0) [17]. This convolutional encoder has 8-states according to the content of these cells as follows:

SR = SR^2, SR^1, SR^0

State = 0 0 0, 0 0 1,.., 1 1 1

State = 0, 1,….., 7

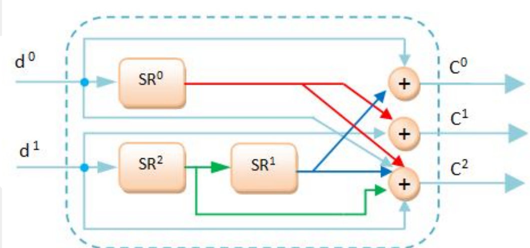

Figure 4 Example of Paaske's non-recursive convolutional encoder

After each encoding process, a new codeword (c) is generated depending on the new dataword (d) of the input sequence and the previous state of the memory cells. A new state of the memory cells is generated depending on the new dataword of the input sequence. Table 1 shows the generated codeword and the related state of the memory cells after each encoding process. For example, if the dataword of input sequence is d = (d^1, d^0) = (1, 0) = 2 and if the state of cells is SR = (SR^2, SR^1, SR^0) = (1, 0, 0) = 4 thus after one time slot, the new state of the cells will be SR = (SR^2, SR^1, SR^0) = (1, 1, 0) = 6 and the new generated codeword will be c = (c^2, c^1, c^0) = (0, 1, 0). Hence, if the sequence of information bits is d= {10 11 10 11 01} with assuming that the rightmost bit is the first input bit, thus the datawords of input sequence are {2 3 2 3 1}. Before the encoding process, the state of memory cells is initialized to zero. So, when the first dataword of the information source d(1) = 1 arrives to the encoder, the first codeword c(1) = 5 is generated after one time slot at the output of the encoder and the state of cells is changed from State "0" to State "1". When the second dataword of the information source d(2) = 3 arrives to the encoder, the second codeword c(2) = 5 is generated after the second time slot and the state of cells is changed from State "1" to State "5". The encoding process is done for all datawords of the information source in the same manner and the generated codewords will be as follows c = {1 2 4 5 5}, also the states of the cells will be as follows State = {6 7 6 5 1 0}. The outputs of convolutional encoder are interleaved randomly by using S-random bit-interleavers as shown in Fig. 1. The interleaved bits are labeled to 8-PSK Gray constellation to generate complex symbols.

State (SR^2, SR^1, SR^0)	Information Word d= (d^1, d^0)			
	00=1	01=1	10=2	11= 3
000=0	000=0	101=5	110=6	011=3
00 =1	110=6	011=3	000=0	101=5
010=2	101=5	000=0	011=3	110=6
011=3	011=3	110=6	101=5	000=0
100=4	100=4	001=1	010=2	111=7
101=5	010=2	111=7	100=4	001=1
110=6	001=1	100=4	111=7	010=2
111=7	111=7	010=2	001=1	100=4
State (SR^2, SR^1, SR^0)	Codeword c= (c^2, c^1, c^0)			
000=0	000=0	001=1	100=4	101=5
001=1	000=0	001=1	100=4	101=5
010=2	000=0	001=1	100=4	101=5
011=3	000=0	001=1	100=4	101=5
100=4	010=1	011=3	110=6	111=7
101=5	010=1	011=3	110=6	111=7
110=6	010=1	011=3	110=6	111=7
111=7	010=1	011=3	110=6	111=7
Next State = (SR^2, SR^1, SR^0)				

Table 1 The Generated Codeword and the Related State of the Encoder's Cells After Each Encoding Process

2.4 BICM with Iterative Decoding

In spite of improving the performance of Ungerbock's TCM scheme by maximizing the minimum Hamming distance as proposed in Zehavi's BICM scheme, but this improvement is still limited to AWGN channel because the free Euclidean distance (FED) between the coded symbols is still low. Li and Ritcey proposed new scheme using the iterative decoding process in BICM scheme (BICM-ID) to improve the performance on Rayleigh fading channel [6, 7]. The system performance is improved by taking advantage of using Gray labeling at the transmitter side and using the iterative decoding process at the receiver side. The iteration process makes the soft information which comes back from the convolutional decoder to the demodulator more reliable after each iteration process.

2.4.1 Labeling process

This section shows the mapping of encoded bits to the constellations' points of the 8-PSK modulator. Fig. 5 illustrates the process of partitioning the interleaved encoded bits to subsets according to the three bits' positions in the constellation for set partitioning (SP) and Gray labeling methods [18]. As shown in Fig. 5, there are two subsets $X(i,1)$ and $X\ (i,0)$, i = 0, 1, 2, where i refers to one of the three bits' positions for 8-PSK symbols. The positions of the bits in the subset $X(i,1)$ are represented by the shaded areas, while in the subset $X(i,0)$ are represented by the unshaded areas. These shaded and unshaded areas are considered as decision areas for each bit assigned to a symbol. The hard-decision demodulation process in BICM scheme depends on these areas to detect each bit of the symbol. Both Gray and SP labeling methods have the same Euclidean distance between the transmitted symbols. Each method has a different number of nearest neighbors. For instance the subset $X(1,1)$ refers to the area where bit-1 equal to 1, where it has one area with regard to the Gray labeling method as shown in Fig. 5 (a). On the contrary, with regard to the SP labeling method, the subset $X(1,1)$ is divided into two areas as shown in Fig. 5 (b). Therefore, it is obvious that the Gray labeling method has less number of nearest neighbors than the SP labeling method. For the latter when the number of nearest neighbors is large, it increases the probability of decoding error. Thus, the Gray labeling method is considered as a more suitable mapping of the bits for BICM without iteration [18] as shown in Fig. 3.

During the iterative decoding process in BICM-ID scheme, the feedback information Bit 1 and Bit 2 are used to compute the a-priori probability for the constellation relate to Bit 0 because they represent the original information bits as shown in Fig. 2. The constellation relates to Bit 0 is limited to pairs of points in the constellation as shown in the right part of Fig. 6. In the same manner, the a-priori probabilities for the constellation relate to Bit 1 and Bit 2 are computed depending on the feedback information about the other two bits. Therefore the 8-PSK constellation can be expressed as 4 BPSK constellations for each of Bit 0, Bit 1, and Bit 2 [19].

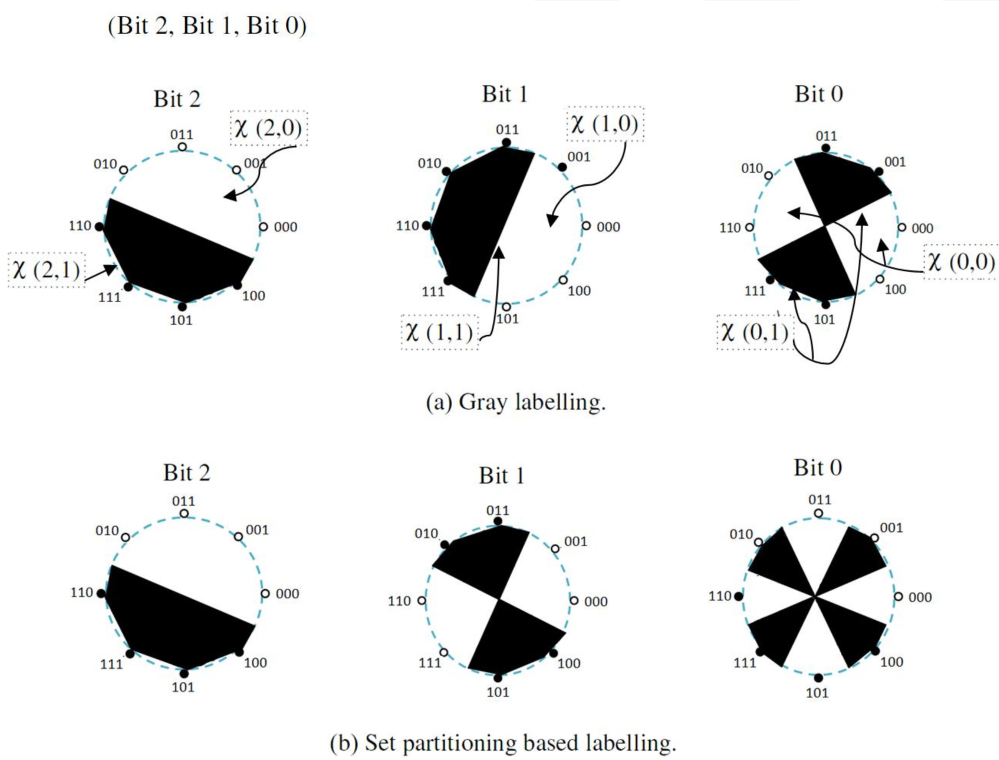

Figure 5 The process of partitioning the interleaved encoded bits to subsets for both labeling methods [7]

The performance of BICM-ID scheme can be optimized during each iterative decoding process by maximizing the minimum Euclidean distance between the two points of four pairs at all the constellations related to Bit 2 (the left), Bit 1 (the center), Bit 0 (the right) of Fig. 6 (a).

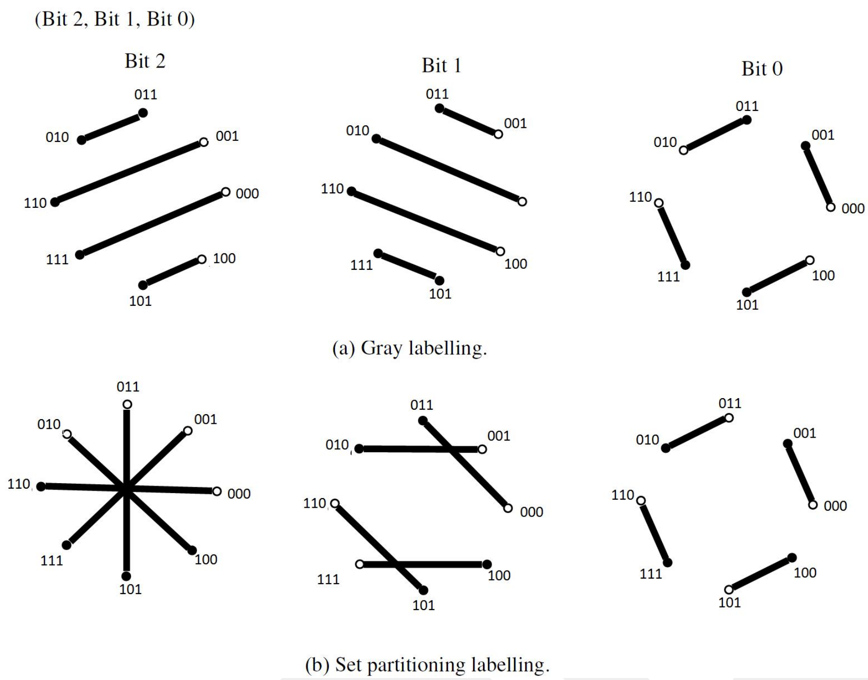

Figure 6 The minimum Euclidean distance between the 2-points of all pairs in the 8-PSK constellation for both labeling methods

The SP labeling method is better than Gray labeling method. The SP labeling method provides high minimum Euclidean distances between symbol sequences than a Gray labeling method for Bit 1 and Bit 2 as shown in the left and center parts of Fig. 6 (b). The performance of the first iteration of BICM-ID scheme is very important, since it is necessary to prevent the increase in error propagation due to occur the errors in feedback information bits. The propagation of error in the received bits can be controlled effectively depending on the soft decision feedback of the convolutional decoder. Thus, the SP labeling method is preferred to use at BICM-ID scheme [18, 19].

For instance to achieve high Euclidean distance between the two points of all pairs at the constellation relate to Bit 2 as shown in Fig. 6 (b), the values of Bit 0 and Bit 1 must be decoded correctly and returned to the SP labeling demodulator. If the values of Bit 0 and Bit 1 are not decoded correctly, the requested Euclidean distance between symbol sequences at the constellation relate to Bit 2 will not be high and lead to occur errors propagation in the received bits. From the other side, if the Hamming distance between the codewords generated by ideal convolutional encoder is high, these convolutional codes have the capability to decode the received bits correctly. The use of ideal convolutional codes with suitable labeling method have the capability to convert the maximum Hamming distance between the generated codewords into a maximum Euclidean distance between the two points of all pairs at the constellations shown in Fig. 6.

In brief, BICM-ID scheme uses m independent bit interleavers to rearrange the order of bits sequence and generate m independent parallel streams. It uses 2^m labelling scheme to convert the independent parallel streams to complex signals. Also it uses an iterative decoding process to reduce the bit error rate. The use of m independent bit interleavers is to improve system performance on a Rayleigh fading channel by increasing the diversity gain. The use of the SP labeling method and iterative decoding process is to improve the system performance over AWGN and Raleigh fading channels by increasing FED between the symbol sequences. Hence, BICM-ID is considered as a powerful scheme because it combines between the perfect binary codewords and the efficient bandwidth provided by M-ary Modulator [18, 19].

2.4.2 Design of interleavers

The performance of BICM-ID scheme can be improved by using the perfect design of interleavers such as Block interleavers, Helical interleavers, Random interleavers and S-Random interleavers. Li and Ritcey imposed restrictions on the interleaver's design to maintain high Euclidean distance between the two signal points of all pairs in BPSK constellations. In this thesis S-random interleaver is used, where three independent S-random interleavers are designed with M-ary modulator. The designed interleavers are generated independently and randomly. The error propagation caused by the correlation over a fading channel will be distributed randomly and effectively by using separated bit interleavers. This results in better performance over Rayleigh fading channels at the expense of little degradation in the system performance over AWGN channels [16, 20].

The objectives of the design of the S-random interleaver used in this thesis are:-

1) To improve the performance of the system over Rayleigh fading channel by increasing the diversity order through partitioning the correlation that may occur between the transmitted bits or that may occur in the environment of the Rayleigh fading channel.

2) To reduce the effect of error propagation in the received bits that may occur due to the feedback during the iteration process of demodulation and decoding.

The purpose of the interleaver is illustrated in Fig. 7, where the first row represents a stream of bits in the original sequence, while the second row represents rearrange the order of bits sequence by using Random interleaver [21]. A burst of noise may appear in the fading channel affects on one or more bits of the stream as illustrated in red color causing concatenated bit errors at the receiver. By using de-interleaving process at the receiver, the concatenated bit errors will be distributed by returning the original order of bits sequence as illustrated in the third row of Fig. 7. This bit error distribution makes easy for the convolutional decoder to correct the bit errors. If the interleaver is not available in the system, the concatenated bit errors will not be distributed which make difficult for the convolutional decoder to correct the bit errors and retransmission is needed.

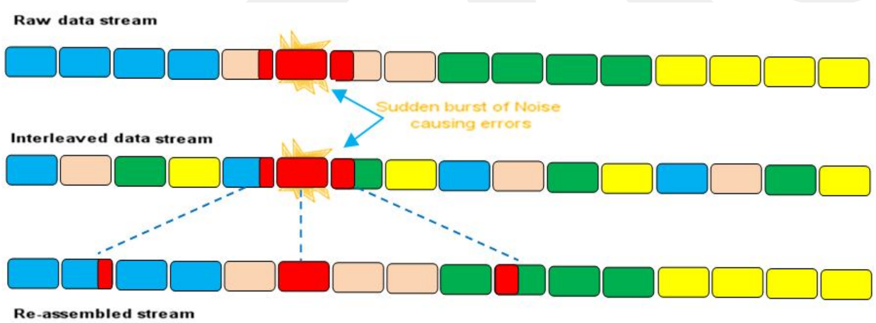

Figure 7 Example illustrates the purpose of the interleaver

2.5 The Operation of BICM-ID Scheme

2.5.1 General description

The structure of BICM-ID system with iterative decoding process (soft-decision feedback) is illustrated in Fig. 8. The transmitter module consists of a non-recursive convolutional encoder with 8-states. The rate of the convolutional encoder equals 2/3. Three independent bit interleavers of type S-random are used. A modulator of type 8-PSK is employed [11]. The receiver module of BICM-ID system consists of 8-PSK demodulator, three bit de-interleavers, and MAP decoder [22]. The MAP decoder has been chosen for SISO model. MAP decoder computes two values of a-posteriori probability, one of them to compute the feedback and the second to make the hard decision to recover the information bits. The demodulation and decoding processes are iterated for sufficient number of times.

The principle of iterative decoding process is to feed back the probabilities to the demodulator input after interleaving them to reduce the effect of error propagation in the received bits through improving the received weak bits [11].

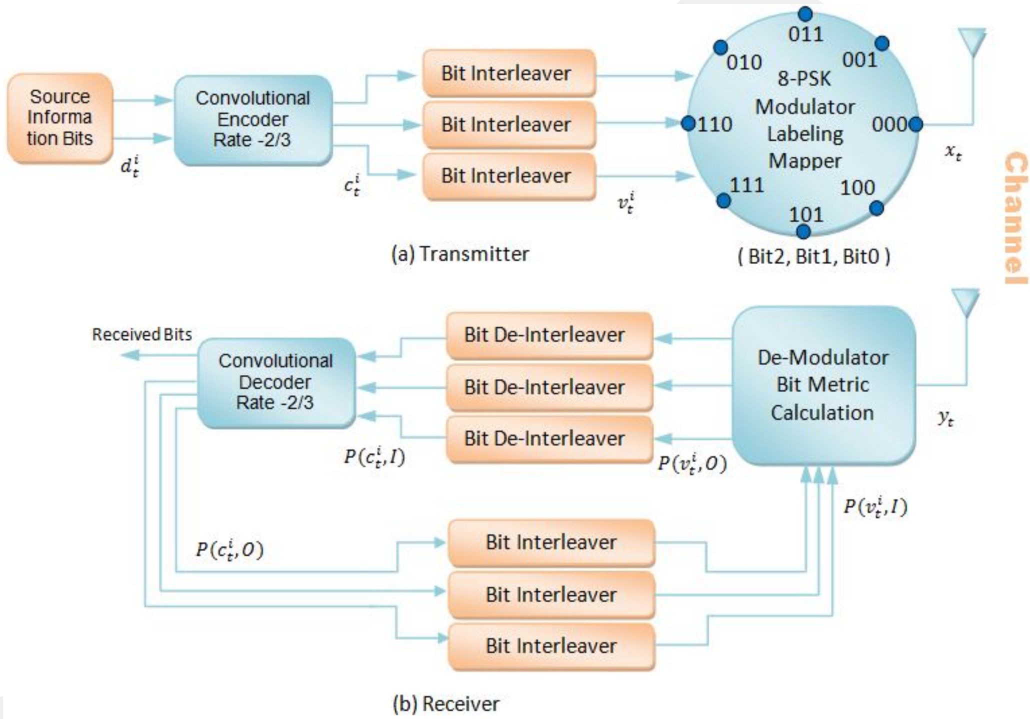

Figure 8 BICM-ID system using iterative decoding

2.5.2 Transmitter module

The transmitter module of BICM-ID system is illustrated in Fig. 8 (a). The input pair to the convolutional encoder is denoted by:

$$d_t = [d_t^0, d_t^1] \qquad (2.3)$$

The bit groups at the output of convolutional encoder are denoted by:

$$c_t = [c_t^0, c_t^1, c_t^2] \qquad (2.4)$$

where c_t^i represent the ith bit in a symbol at each time slot 't' as defined in Table 1. Each output of convolutional encoder is interleaved by using independent S-random bit interleavers [11]. The interleaved bits are grouped together at each time slot 't' using a 8-PSK modulator to form the bits groups given:

$$v_t = [v_t^0, v_t^1, v_t^2] \tag{2.5}$$

Next, each bits group is mapped (labeling process) to a point in the 8-PSK constellation χ according to its binary value. Depending on symbol labels μ in the 8-PSK constellation χ , the complex symbol is chosen as:

$$x_t = \mu(v_t),\ x_t \in \chi \tag{2.6}$$

where χ represents the signals set in the 8-PSK constellation defined as:

$$\chi = \{e^{jn2\pi/8}, n = 0, \dots, 7\} \tag{2.7}$$

The received signals over Raleigh and AWGN channels are represented by:

$y_t = h_t \sqrt{E_s}\, x_t + n_t$ [Received signal over Rayleigh fading channel]

$y_t = \sqrt{E_s}\, x_t + n_t$ [Received signal over AWGN channel] (2.8)

where h_t represents the fading amplitude with Rayleigh distribution [24] and variance '1' (the real and imaginary coefficients of the Rayleigh fading have a variance equals '0.5'). The fading amplitude is assumed to remain constant along each frame. Let E_s represent the transmitted energy per symbol. For BICM system which consists of a convolutional encoder with rate-2/3, the energy per bit equals $E_b = E_s/2$. n_t represents a complex noise of type additive white Gaussian noise. The real and imaginary parts of the complex noise have a variance equals '0.5' ($\sigma_I^2 = \sigma_Q^2 = N_\circ/2$). The Rayleigh channel coefficients have $\mathrm{E}(h_t^2) = 1$. In this thesis, we assumed that there is an ideal channel side information (CSI) [25] at the receiver module, where the fading amplitude is estimated perfectly and the receiver knows the fading coefficients.

2.5.3 Receiver module

The receiver module of BICM-ID system is illustrated in Fig. 8 (b). The demodulator receives the faded complex symbol from the channel and computes six bit metrics. Then these bit metrics are de-interleaved and sent to the decoder. The decoder computes the transition metrics in order to make the decision and restore the original information bits by computing the likelihood metrics [11].

2.5.4 Demodulation process

The 8-PSK demodulator receives the faded symbols and computes six bit metrics for each received symbol [11, 26]. The bit metrics are computed as:

$$P\left(v_t^i = b \mid y_t\right) \approx \sum_{x_t \in \chi(i,b)} P\left(x_t / y_t, p_t\right) \approx \sum_{x_t \in \chi(i,b)} P\left(y_t / x_t, p_t\right) P\left(x_t\right) \tag{2.9}$$

where i takes values from the set {0, 1, 2}, b takes one of the values {0, 1}, $x_t = \mu(v_t)$ represents the signals' set in the 8-PSK constellation and $P(x_t)$ represents the a-priori probability of each symbol in the constellation. During the first iteration, the a-priori probabilities are assumed to have the same values for all the symbols in the constellation. However, in the other iterations the a-priori probabilities are updated depending on the soft information fed from the convolutional decoder.

The probability of the transmitted symbol over an AWGN channel is written as [11, 26]:

$$P(y_t / x_t, h_t) = \frac{1}{2\pi\sigma^2}\, exp\left[-\frac{|y_t - x_t|^2}{2\sigma^2}\right] \tag{2.10}$$

where the constant factor ($\frac{1}{2\pi\sigma^2}$) can be neglected leading to the equation:

$$P(y_t / x_t, h_t) = exp\left[-\frac{|y_t - x_t|^2}{2\sigma^2}\right] \tag{2.11}$$

The probability of the transmitted symbol over a fading channel is given as:

$$P(y_t/x_t, h_t) = \frac{1}{2\pi\sigma^2}\ exp\left[-\ \frac{|y_t - h_t\ x_t|^2}{2\sigma^2}\right] \tag{2.12}$$

Furthermore, the demodulation process is the process of de-mapping the bits, where the received symbols are recovered to its binary values $[\nabla^0\ (x_t), \nabla^1\ (x_t), \nabla^2\ (x_t)]$ as they were before the modulator [11, 26].

The subset $\chi\ (i, b)$ can be written as:

$$\chi\ (\ i, b) =\ \{\mu(\ [\ \nabla^0(x_t), \nabla^1(x_t), \nabla^2(x_t)])|\nabla^j(x_t) \in \{0,1\},\ j\ \neq i\ \} \tag{2.13}$$

Each subset contains all the points (signals) in the 8-PSK constellation which holds the following values $\nabla^i\ (x_t) = b$. In 8-PSK constellation, the number of bits assigned to each symbol equals $m = 3$, thus each subset $\chi\ (i, b)$ consists of $2^m - 1 = 4$ terms as illustrated in Fig. 5. The computations of a-priori probabilities are dependent on the probabilities of two bits out of three bits assigned for each symbol. These a-priori probabilities are taken into consideration in each iteration process when computing the bit metrics for each received symbol.

Depending on Benedetto's blogging [27], the original information bit d_t^i at position index i and time index t, has a-priori probabilities $P(d_t^i = 0; I)\ and\ P(d_t^i =\ 1; I)$ refer to being 0 or 1 sequentially, where I denotes the a-priori probability of the bit. This blogging can be simplified to $P(d_t^i; I)$ as illustrated in Fig. 8. In similar manner, the coded bit c_t^i, which is at position index i and time index t has a-priori probabilities $P(c_t^i; I)$ for simplicity. Each of the original bits (d_t^i) and the coded bits (c_t^i) have a-posteriori probabilities information (APP) $P(d_t^i; O)$ and $P(c_t^i; O)$ sequentially, where O denotes the a-posteriori probability of the bit.

In the first iteration process, the a-priori probabilities $P(x_t)$ are not computed and assumed equal $(1/2^m)$. Then the a-posteriori probabilities of the original transmitted bits $P(d_t^i, O)$ are computed by using the MAP decoder. Also the MAP decoder computes the a-posteriori probabilities of the coded bits $P(c_t^i, O)$ depending on bit metrics probabilities $P(v_t^i = b/O)$ after de-interleaving them as illustrated in Fig. 8

(b) doesn't exist, thus it will not take into consideration in the computations of the whole decoding process [26, 27].

In all iterative decoding processes the a-posteriori probabilities of the coded bits $P(c_t^i;\ O)$ are interleaved, then the interleaved a-posteriori probabilities $P(v_t^i;\ I)$ are fed back to the demodulator input as illustrated in Fig. 8 (b). These independent interleaved probabilities are used to compute the a-priori probabilities for each symbol $x_t \in \chi$ as follows:

$$\begin{aligned} P(x_t) &= P(\mu\,[\,\nabla^0(x_t), \nabla^1(x_t), \nabla^2(x_t)\,]) \\ &= \textstyle\prod_0^2 P(\,v_t^i = \nabla^j\,(x_t)\,;\,I) \end{aligned} \tag{2.14}$$

where $\nabla^j\,(x_t) \in \{0,1\}$ represents one of the three bits assigned to each symbol x_t in the 8-PSK constellation through labeling process. After computing the a-priori probabilities $P(x_t)$ for all transmitted symbols x_t, thus in all the iterative decoding processes which following the first iterative decoding process, the bit metrics (a-posteriori probabilities APP) are computed for all received symbols by using Eq. (2.10) and Eq. (2.14) as follows [26, 27]:

$$\begin{aligned} P(v_t^i = b; O) &= \frac{P(v_t^i = b \mid y_t)}{P(\ v_t^i = b; I)} \\ &= \frac{\left(\sum_{x_t \in \chi(i,b)} P(y_t / x_t, p_t) P(x_t)\right)}{P(v_t^i = b; I)} \\ &= \sum_{x_t \in \chi(i,b)} P(y_t / x_t, p_t) \prod_{j \neq i}^{2} P(v_t^j = v^j(x_t)\ ;\ I) \quad i = 1,2,3; b = 0,1 \end{aligned} \tag{2.15}$$

As observant from Eq. (2.15), the computations of bit metrics for each received symbol are recalculated in all iteration processes depending only on the a-priori probabilities of two bits out of three bits assigned to the symbol. These a-priori probabilities are updated in each iteration process by making a feedback connection between the convolutional decoder and the demodulator. The updated bit metrics are sent to the convolutional decoder and the iteration process continues several times between the decoder and the demodulator. In the last iteration process, the a-posteriori probabilities of the original information bits $P(d_t^i, O)$, are computed to recover the transmitted information bits.

2.5.5 Decoding process

The type of SISO decoder used in the receiver module of BICM-ID scheme is MAP decoder. As illustrated in Fig. 8 (b), the MAP decoder receives six bit metrics for each received symbol from the demodulator. Depending on the bit metrics and using the Viterbi algorithm, the MAP decoder computes the branch transition metrics for all states of trellis diagram. In MAP decoder forward transition metrics, backward transition metrics, and max likelihood metrics are computed depending on the computed branch transition metrics. These metrics are used to make the decision to recover the original information bits and to compute the soft-decision feedback during all iterative decoding processes.

The algorithm of the MAP decoder was proposed by Raviv, Cocke and Bahle at 1974 [22, 27] to estimate the values of a-posteriori probabilities (APP) for noisy channels. The MAP algorithm can be used to decode the convolutional and block codes.

The MAP algorithm computes three probabilities $\alpha_k(s)$, $\gamma_k(s',s)$ and $\beta_k(s)$, where $\alpha_k(s)$ represents the probability of being in the previous state (s') and transit to the present state (s) (forward transition metric), $\gamma_k(s',s)$ represents the probability of the branch transition between the previous state and the present state, $\beta_k(s)$ represents the probability of being in the present state (s) and transit to the previous state (s') (backward transition metric).

In order to compute all the probabilities $\alpha_k(s)$, $\gamma_k(s',s)$, $\beta_k(s)$ and the a-posteriori probabilities, all the branch transitions between any two states in the trellis diagram should symbolize using two sets of binary numbers. One of these sets lies in the left side represents the input of the convolutional encoder, the second sets lies in the right side represents the output of the encoder as illustrated in Fig. 9.

2.5.5.1 Computation of branch transition metrics $\gamma_k(s',s)$

The value of $\gamma_k(s',s)$ represents the probability of branch transition between the previous state (s') and the present state (s) in each column of the trellis diagram. The computation of $\gamma_k(s',s)$ is considered as the basic computation in the MAP decoder to extract the original information bits from the received symbols [22, 29]. Initially, the MAP decoder receives six bit metrics for each received symbol from the demodulator after de-interleaving them to its original order by using de-interleaver. Then the MAP decoder chooses three out of six received bit metrics according to the binary value of the decoder output put on each branch transition. The values of $\gamma_k(s', s)$ for all branch transitions in the trellis diagram are computed for all received symbols in log-domain as follows:

$$\tilde{\gamma}_k(s', s) = P(c_t^0, I) + P(c_t^1, I) + P(c_t^2, I) \tag{2.16}$$

where $P(c_t^i, I)$ represent the received bit metrics from the demodulator after the process of de-interleaving.

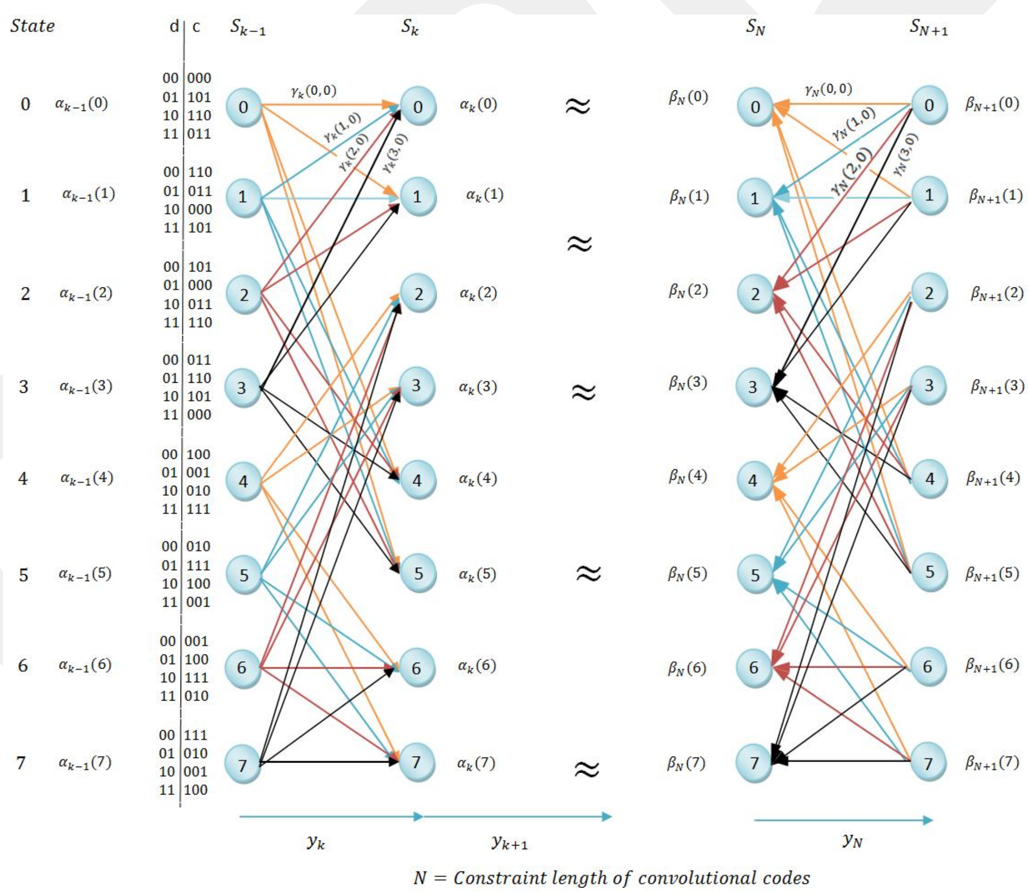

Figure 9 The symbol-based trellis diagram used in the MAP decoder.

2.5.5.2 Computation of forward transition metrics $\alpha_k(s)$

The value of $\alpha_k(s)$ represents the probability of being in state (s) in the trellis diagram. The computation of $\alpha_k(s)$ for each state in the trellis diagram depends mainly on the branch metric $\gamma_k(s', s)$ and the forward metric for the previous state $\alpha_{k-1}(s')$ [22, 29]. The computation of forward state metrics in log-domain is given as:

$$\tilde{\alpha}_k(s) = \max_{s'}{}^{*}\left[\tilde{\alpha}_{k-1}(s') + \tilde{\gamma}_k(s', s)\right] \tag{2.17}$$

where $\tilde{\gamma}_k(s', s)$ represents the branch metric between the previous state and the present state in log-domain, $\tilde{\alpha}_{k-1}(s')$ represents the forward metric for the previous state. Initially, the initial state of the trellis is assumed to be zero in the first stage of the trellis diagram. The initial value of the forward metric in the first stage of the trellis is assumed to be 1 for the zero state and to be 0 for the other states.

2.5.5.3 Computation of backward transition metrics $\beta_k(s)$

The value of $\beta_k(s)$ represents the probability of being in state (s') in the trellis diagram. The computation of $\beta_{k-1}(s')$ for each state in the trellis depends mainly on the value of branch metric $\gamma_k(s', s)$ and the value of backward metric for the previous state $\beta_k(s)$ [22, 29]. The backward state metrics are computed in log-domain as follows:

$$\tilde{\beta}_{k-1}(s') = \max_{s}{}^{*}\left[\tilde{\beta}_k(s) + \tilde{\gamma}_k(s', s)\right] \tag{2.18}$$

where $\tilde{\gamma}_k(s', s)$ represents the branch metric between the previous state and the present state in log-domain, $\tilde{\beta}_k(s)$ represents the backward metric for the previous state. We assumed that the trellis is terminated, so the last state of the trellis is assumed to be zero state. The initial value of the backward metric in the last stage of the trellis is assumed to be 1 for the zero state and to be 0 for the other states. When the MAP decoder completes the computations of branch transition, forward, and backward metrics for all the received symbols, then it computes all the a-posteriori probabilities in each column of the trellis diagram as follows:

$$\text{APPs} = \alpha_{k-1}(s') + \gamma_k(s',s) + \beta_k(s) \tag{2.19}$$

2.5.5.4 Computation of max likelihood metrics $L(d_k)$

The Computation of the max likelihood metrics represents the process of splitting the values of a-posteriori probabilities in each column of the trellis diagram into groups according to the binary input of the convolutional encoder put on each branch transition. Then, the a-posteriori probabilities in each group are summed together. A comparison between the products of summation for all groups is done to choose the greater one [22, 29]. Checking the binary inputs of the convolutional encoder put on the branch transitions which having greater products of summation, where these binary inputs represent the original information bits. The Computation of max likelihood metrics in log-domain is given as:

$$L(d_k) = \max_{D^+}{}^{*}\left[\tilde{\alpha}_{k-1}(s') + \tilde{\gamma}_k(s',s) + \tilde{\beta}_k(s)\right] - \max_{D^-}{}^{*}\left[\tilde{\alpha}_{k-1}(s') + \tilde{\gamma}_k(s',s) + \tilde{\beta}_k(s)\right] \tag{2.20}$$

2.5.5.5 Computation of soft-decision feedback metrics

The Computation of the soft-decision feedback metrics represents the process of splitting the values of a-posteriori probabilities in each column of the trellis diagram into groups according to the binary output of the convolutional encoder put on each branch transition. Then, the a-posteriori probabilities in each group are summed together. The products of summation for all groups represent the soft-decision feedback metrics which are returned to the demodulator after de-interleaving them in each iteration process. The Computation of soft-decision feedback metrics in log-domain is given as:

$$P(c_t^i, O) = max^*\left[\tilde{\alpha}_{k-1}(s') + \tilde{\gamma}_k(s',s) + \tilde{\beta}_k(s)\right] \qquad i = 0,1,2 \tag{2.21}$$

CHAPTER 3

CONCATENATED STRUCTURE FROM BICM AND STBC WITH ITERATIVE DECODING

3.1 Introduction

In mobile communication systems, a predominant way for adapting with the randomness of fading channel is to use more than one antenna either at the transmitter or the receiver or both called MMO systems (multiple-inputs and multiple-outputs systems). The MIMO system increases the diversity gain (spatial and coding diversity) in the wireless communications through transmitting multiple copies of each symbol using multiple antennas over fading channels [4, 30].

The two types of the space-time codes (STC) in MIMO systems are space-time trellis codes "STTC" and space-time block codes "STBC". Both schemes can provide high spatial diversity. However, STBC provides coding gain less than STTC. STBC is considered more appropriate for practical systems because its complexity and cost are less than STTC.

The coding gain provided by STBC scheme is low [5, 31] and in order to achieve maximum coding gain in addition to spatial gain, suitable coded modulation schemes can be concatenated with STBC scheme to improve the performance. Bit-interleaved coded modulation with iterative decoding (BICM-ID) scheme proposed by Li and Ritcey can be concatenated with STBC to form BI-STC-ID which was introduced in [6, 32].

In practical mobile systems, the transmitter model of the joint structure (BI-STC-ID) is a concatenated structure involving a binary outer encoder, bit interleavers, modulator (Mapper), symbol interleaver and an inner STBC encoder to protect the transmitted data over Rayleigh fading channels. The receiver module involves STBC decoder, symbol de-interleaver, demodulator, bit de-interleavers, and MAP decoder which are run in an iterative manner.

3.2 Classical Technique of Maximum Ratio Combining (MRC)

An introduction of the classical maximum ratio combining (MRC) technique is found in [5, 34]. In traditional communication system, a single antenna at the transmitter and receiver is used. If the channel between the transmitter and the receiver is a fading channel, the transmitted symbols may suffer from amplitude fluctuations and phase rotation. To overcome the problems of fading channel, several receivers can be used to receive several copies of the same transmitted symbol. So even if the received symbol from the direct path is faded severely, there is still a chance to receive another copy of the same symbol with low fading from other paths. However, all the received symbols from different paths should be combined with each other at the receiver side. This combination leads to increase the complexity of the system. In practice, the classical MRC technique is used to combine the received symbols.

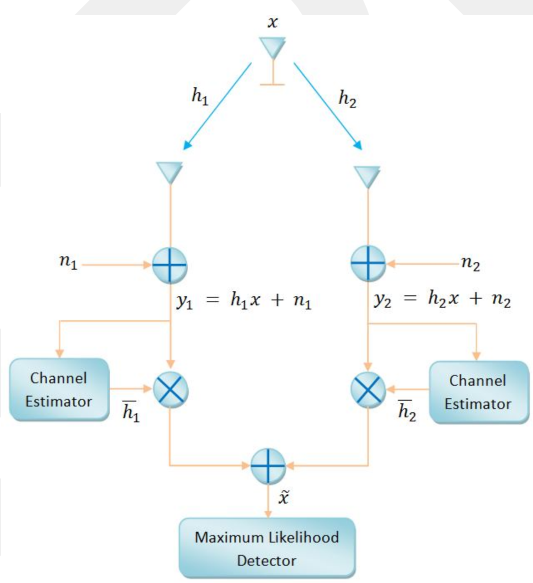

Figure 10 Classical MRC technique with one transmitter and two receivers

The classical MRC technique is represented by a system consists of two receivers as illustrated in Fig. 10. For instance if the symbol x is transmitted, then the transmitted symbol x will propagate over two independent faded channels h_1, h_2 as shown in Fig. 10. For simplicity, the number of propagation paths in each independent channel is assumed to be 1 [5, 34]. Each propagation path is represented by the magnitude and phase denoted as:

$$h_1 = |h_1| e^{j\theta 1} \quad (3.1)$$

$$h_2 = |h_2| e^{j\theta 2} \quad (3.2)$$

where $|h_1|$ *and* $|h_2|$ represent the magnitude distortion of the fading channel, θ_1 and θ_2 represent the phase distortion of the fading channel. Also an additive white Gaussian noise is added to the transmitted faded symbols by the channel, so the received signal will be as follows:

$$y_1 = h_1 x + n_1 \quad (3.3)$$

$$y_2 = h_2 x + n_2 \quad (3.4)$$

where n_1, n_2 represent complex noise. The received signals can be represented in the matrix form as:

$$\begin{pmatrix} y_1 \\ y_2 \end{pmatrix} = x \begin{pmatrix} h_1 \\ h_2 \end{pmatrix} + \begin{pmatrix} n_1 \\ n_2 \end{pmatrix} \quad (3.5)$$

In order to remove the effect of the fading channel, we assumed that there is a perfect channel estimator at the receiver which means that the receiver has the exact knowledge of the complex coefficients of fading channels. The received signals y_1 *and* y_2 are multiplied by the conjugate of the complex coefficients of the fading channel $\bar{h}_1$*and* $\bar{h}_2$ sequentially. At the input of the maximum likelihood detector (MLD), the two received signals are combined after removing the effect of fading channels as follows:

$$\begin{aligned} \tilde{x} &= \bar{h}_1 y_1 + \bar{h}_2 y_2 \\ &= \bar{h}_1 h_1 x + \bar{h}_1 n_1 + \bar{h}_2 h_2 x + \bar{h}_2 n_2 \\ &= (|h_1|^2 + |h_2|^2)\, x + \bar{h}_1 n_1 + \bar{h}_2 n_1 \end{aligned} \quad (3.6)$$

The maximum likelihood detector (MLD) receives the combined signals and computes all the Euclidean distances between the combined signal $\tilde{x}$ and all the possible transmitted signals. Then, MLD makes the decision to recover the original symbols by choosing the minimum Euclidean distance computed previously.

3.3 Space Time Block Code (STBC) Using Two Transmitters

Two receiver antennas are used to provide two independent faded copies of the same transmitted symbol at the receiver. The STBC technique is used in the concept of transmitter diversity rather than receiver diversity.

The transmitter diversity with STBC can be achieved by transmitting two independent copies of the same symbol by two transmitter antennas spaced from each other a sufficient distance rather than using two receiver antennas. If one of the transmitted copies is faded over the fading channel, the other transmitted copy may be reached to the receiver with high power.

The system which uses the transmitter diversity will transmit each symbol twice, each once is transmitted by one of the transmitter antennas. The two transmitted copies of each symbol superimpose on each other and with the help of the receiver, the two transmitted copies will be extracted from the received signal. In order to circumvent on the previous problem, Alamouti proposed a simple solution from the conceptual and executive side [5, 32]. He found that the most successful method to transmit the two independent copies of the same symbol by two antennas is through using the system outlined below. In more details, the transmission matrix which has used in Alamouti's approach [5, 32] is defined as:

$$G_2 = \begin{pmatrix} x_1 & x_2 \\ -\bar{x}_2 & \bar{x}_1 \end{pmatrix} \quad (3.7)$$

where the transmitted symbols in the second row of the transmission matrix contain bar above them which refers to their conjugate version. From Eq. (3.7), we notice that the transmitted symbol x_1 and its copy are not transmitted at the same time by the two transmitter antennas to avoid the superposition between them at the input of the receiver. Each symbol and its copy are transmitted by two different transmitter antennas and during two intervals of the symbol. The independent copy of the transmitted symbol x_1 is transmitted after computing its conjugate value. Transmitting two copies of each symbol leads the transmission rate to decrease to the half.

The transmission matrix G_2 in Eq. (3.7) consists of two columns and two rows. The number of columns represents the number of transmitter antennas $p = 2$ and it also represents the number of input symbols. The number of rows represents the number of time slot used for transmission. The encoding rate of STBC scheme according to transmission matrix in Eq. (3.7) equals $k/n = 1$. The processes of encoding and transmission relating to STBC scheme are illustrated in Table 2, where every two signals are transmitted together for each time slot [31, 32]. One of the signals is transmitted by the antenna Tx_1 while the other signal is transmitted by the antenna

Tx_2. For instance, the signals x_1 *and* x_2 are transmitted together from the antennas Tx_1 *and* Tx_2 sequentially at the first time slot $T = 1$. The following two signals $-\bar{x}_2$ *and* $\bar{x}_1$, which represent the conjugate values of the signals x_1 *and* x_2 sequentially are transmitted together from the antennas Tx_1 *and* Tx_2 sequentially at the second time slot $T = 2$.

Time slot, T	Antenna	
	Tx_1	Tx_2
1	x_1	x_2
2	$-\bar{x}_2$	$\bar{x}_1$

Table 2 The Processes of the Encoding and Transmission Relating to STBC [32]

3.4 STBC Using Two Transmitters & One Receiver

The signals transmitted by STBC according to the transmission matrix G_2 in Eq. (3.7) can be decoded using the decoding approach employed for one receiver. Using a similar approach decoding the space time block code can be done using an arbitrary number of receivers. The basic representation of the STBC scheme which consists of two transmitters and one receiver is shown in Fig. 11. The symbols are encoded and transmitted according to the transmission matrix G_2 in Eq. (3.7). It is clear from the figure that each two symbols are transmitted at the same time by using the two transmitter antennas Tx_1 *and* Tx_2 [31, 35]. As previously mentioned, we assumed that the fading amplitude is constant along two successive time slots. So, the independent fading channels can be written as:

$$h_1 = h_1\,(T = 1) = h_1(T = 2) \tag{3.8}$$

$$h_2 = h_2\,(T = 1) = h_2(T = 2) \tag{3.9}$$

Also an independent complex noise is added to the transmitted signal over the fading channel. So, the received faded signals will be as follows:

$$y_1 = h_1 x_1 + h_2 x_2 + n_1 \tag{3.10}$$

$$y_2 = -h1\,\bar{x}_2 + h2\,\bar{x}_1 + n_2 \tag{3.11}$$

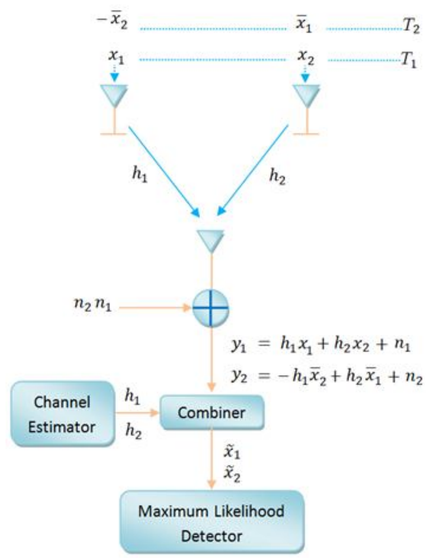

Figure 11 Basic representation of the STBC consisting of two transmitters and one receiver

where y_1 *and* y_2 represent the first and second received signals respectively. From Eq. (3.10) and Eq. (3.11), it is obvious that the received signal y_1 consists of the transmitted signals x_1 *and* x_2 and the received signal y_2 consists of the transmitted conjugate signals $\bar{x}_1$ *and* $\bar{x}_2$. At the receiver, the transmitted signals x_1 *and* x_2 are extracted from the received faded signals y_1 *and* y_2. The two received faded signals are sent to the combiner as illustrated in Fig. 11. With the help of the perfect channel estimator, the combiner performs a simple signal processing to extract the transmitted signals x_1, x_2. The perfect channel estimator means that the receiver has the exact knowledge about the fading channel coefficients h_1 *and* h_2 [31, 35]. Precisely, the transmitted signal x_1 can be decided from the combination of the two received faded signals y_1 *and* y_2 given as:

$$\begin{aligned}\tilde{x}_1 &= \bar{h}_1\, y1 + h2\, \bar{y}_2 \\ &= \bar{h}_1 h_1 + \bar{h}_1 h_2 x_2 + \bar{h}_1 n_1 - h_2 \bar{h}_1 x_2 + h_2 \bar{h}_2 \bar{x}_1 + h_2 \bar{n}_2 \\ &= (|h_1|^2 + |h_2|^2)\, x_1 + \bar{h}_1 n_1 + h_2 \bar{n}_2 \qquad (3.12)\end{aligned}$$

In the same manner, the transmitted signal x_2 can be estimated from:

$$\begin{aligned}\tilde{x}_2 &= \bar{h}_2 y_1 - h_1 \bar{y}_2 \\ &= \bar{h}_2 h_1 x_1 + \bar{h}_2 h_2 x_2 + \bar{h}_2 n_1 + h_1 \bar{h}_1 x_2 - h_1 \bar{h}_2 x_1 - h_1 \bar{n}_2 \\ &= (|h_1|^2 + |h_2|^2)\, x_2 + \bar{h}_2 n_1 + h_1 \bar{n}_2 \qquad (3.13)\end{aligned}$$

Depending on the orthogonality property of the STBC as illustrated in the transmission matrix at Eq. (3.7), the process of extracting the transmitted signal x_1 in Eq. (3.12) doesn't depend on the transmitted signal x_2, so the signal x_2 is removed from Eq. (3.12). The transmitted signal x_1 is also canceled from Eq. (3.13) because of the orthogonality. The two combined signals $\tilde{x}_1$ *and* $\tilde{x}_2$ are sent to the maximum likelihood detector (MLD) as shown in Fig. 11 to restore the transmitted signals. MLD computes the minimum Euclidean distances between each combined signal and all the possible transmitted signals and chooses the transmitted signal which gives maximum Euclidean distance according to this equation:

$$dist(\tilde{x}, x_i) \leq dist(\tilde{x}, x_j), \qquad \forall_i \neq j \tag{3.14}$$

In general, a simple rule can be concluded from Eq. (3.12) and Eq. (3.13) for processing the received faded signal to extract the transmitted signal x_i. Where each received faded signal y_j is considered a linear combination of the transmitted signal x_i multiplied by the fading channel h_i. Also, if the equation of the received signal y_j contains on the transmitted signal x_i, thus this equation is multiplied by the conjugate value of the fading channel $\bar{h}_i$. If the equation of the received signal y_j contains on the transmitted conjugate signal $\bar{x}_i$, thus the value of the fading channel h_i is multiplied by the conjugate value of the received signal $\bar{y}_j$.

3.5 STBC Using Two Transmitters & Two Receivers

The example in section (3.4) illustrates the encoding and decoding processes for STBC using one receiver whose transmission matrix G_2 is given in Eq. (3.7). The same approach can be easily applied to any number of receivers, where the process of encoding and the sequence of transmission are similar to that used in the scheme of single receiver. The STBC which consists of two transmitters and two receivers is illustrated in Fig. 12. The variable i in the notations y_{ij}, h_{ij} *and* n_{ij} refers to the sequence of the receiver [35]. The variable j in the notation h_{ij} refers to the sequence of the transmitter. While the variable j in the notations y_{ij} and n_{ij} refers to the time slot. Depending on the previous assumption there is a virtual fading channel between each transmitter antenna and receiver antenna, so the number of virtual fading channels in the STBC scheme that consists of two transmitter and receiver antennas equals to 4 as illustrated in Fig. 12. The received faded signals at the first receiver Rx_1 after adding an independent complex AWGN to them can be written as follows:

$$y_{11} = h_{11}x_1 + h_{12}x_2 + n_{11} \quad (3.15)$$

$$y_{12} = -h_{11}\bar{x}_2 + h_{12}\bar{x}_1 + n_{12} \quad (3.16)$$

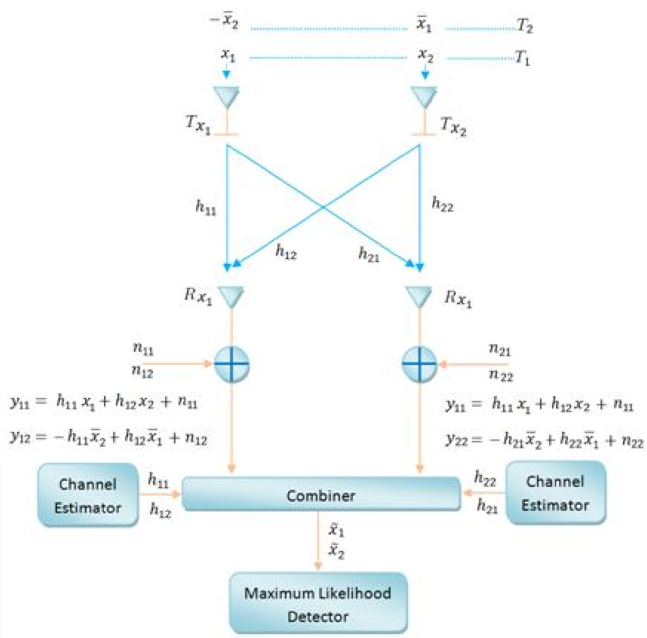

Figure 12 STBC consisting of two transmitters and two receivers

With the same manner, the received faded signals at the second receiver Rx_2 after adding an independent complex AWGN to them can be written as follows:

$$y_{21} = h_{21}x_1 + h_{22}x_2 + n_{21} \quad (3.17)$$

$$y_{22} = -h_{21}\bar{x}_2 + h_{22}\bar{x}_1 + n_{22} \quad (3.18)$$

In other words, the equations of the received faded signals at any receiver can be generalized as follows:

$$y_{i1} = h_{i1}x_1 + h_{i2}x_2 + n_{i1} \quad (3.19)$$

$$y_{i2} = -h_{i1}\bar{x}_2 + h_{i2}\bar{x}_1 + n_{i2} \quad (3.20)$$

where $i = \{1, ..., q\}$ represents the receiver's sequence, and q represents the receiver's number. The received signals y_{11}, y_{12}, y_{21} and y_{22} are combined together to extract the transmitted signals x_1 and x_2 as shown in Fig. 12. The generated combined signals are as follows:

$$\tilde{x}_1 = \bar{h}_{11} y_{11} + h_{12} \bar{y}_{12} + \bar{h}_{21} y_{21} + h_{22} \bar{y}_{22} \tag{3.21}$$

$$\tilde{x}_2 = \bar{h}_{12} y_{11} - h_{11} \bar{y}_{12} + \bar{h}_{22} y_{21} - h_{21} \bar{y}_{22} \tag{3.22}$$

The generated combined signals can be generalized to any number of receivers equals to q as follows:

$$\tilde{x}_1 = \sum_{i=1}^{q} (\bar{h}_{i1} y_{i1} + h_{i2} \bar{y}_{i2}) \tag{3.23}$$

$$\tilde{x}_2 = \sum_{i=1}^{q} (\bar{h}_{i2} y_{i1} - h_{i1} \bar{y}_{i2}) \tag{3.24}$$

The generated combined signals in Eq. (3.21) and Eq. (3.22) can be simplified as follows:

$$\tilde{x}_1 = (| h_{11}|^2 + | h_{12}|^2 + |h_{21}|^2 + |h_{22}|^2) x_1 + \bar{h}_{11} n_{11} + h_{12} \bar{n}_{12} + \bar{h}_{21} n_{21} + h_{22} \bar{n}_{22} \tag{3.25}$$

$$\tilde{x}_2 = (| h_{11}|^2 + | h_{12}|^2 + |h_{21}|^2 + |h_{22}|^2) x_2 + \bar{h}_{12} n_{11} - h_{11} \bar{n}_{12} + \bar{h}_{22} n_{21} - h_{21} \bar{n}_{22} \tag{3.26}$$

The Eq. (3.23) and (3.24) which represent the generated combined signals in the generalized form can be simplified as follows:

$$\tilde{x}_1 = \sum_{i=1}^{q} (|h_{i1}|^2 + |h_{i2}|^2)\, x_1 + \bar{h}_{i1} n_{i1} + h_{i2} \bar{n}_{i2} \tag{3.27}$$

$$\tilde{x}_2 = \sum_{i=1}^{q} (|h_{i1}|^2 + |h_{i2}|^2)\, x_2 + \bar{h}_{i2} n_{i1} + h_{i1} \bar{n}_{i2} \tag{3.28}$$

Finally, the combined signals $\tilde{x}_1$ and $\tilde{x}_2$ are computed and sent to the maximum likelihood detector (MLD) as shown in Fig. 12. The MLD is dependent on Eq. (3.14) to extract the transmitted signals by computing the minimum Euclidean distances between each combined signal and all possible transmitted signals and choose the transmitted signal which gives a maximum Euclidean distance [35].

From Eq. (3.27), we can notice that the transmitted signal x_1 is multiplied with $|h_{i1}|^2 + |h_{i2}|^2$ which represent a product of summation for all the amplitudes of fading channels. Thus, the combined signal $\tilde{x}_1$ will be at high reliability if the fading channel amplitudes are high. In Eq. (3.12) there are two values of the fading channel amplitudes h_1 and h_2 which mean that the transmitted signal x_1 propagates in two independent fading channels to reach the receiver. So, if one of the independent fading channels has an effect on the transmitted signal with high fading, the other independent fading channels may affect with low fading and may provide the transmitted signal with high reliability to restore at the receiver. This explains that the communication system which consists of two transmitters and one receiver has a performance better than the system consists of one transmitter and one receiver. In other words, in the traditional system which consists of one transmitter and one receiver the transmitted signal propagates over single independent fading channel, therefore if this single path has high fading the transmitted signal may attenuate severely. We can notice in Eq. (3.27) that there are four amplitudes of the fading channel h_{11}, h_{12}, h_{21} and h_{22} through which the transmitted signal x_1 and the conjugated signal $\bar{x}_1$ propagate over four independent fading channels to reach the receiver. This leads to increment the reliability given to the combined signals $\tilde{x}_1$, $\tilde{x}_2$ to extract the transmitted signals x_1, x_2.

3.6 Maximum a-Posteriori (MAP) Decoding for STBC Scheme

The new simple rule for decoding called maximum a-posteriori (MAP) is used recently to decode space time block codes introduced by Bauch [36]. The MAP decoder used in STBC scheme provides soft outputs which are symbol probabilities, where these outputs are sent to the concatenated decoder or demodulator to use them as inputs to the following stage. For instance, the channel decoders such as TCM [9], turbo codes and BICM-ID [20] schemes can be concatenated with STBC to improve the system performance.

If there are k-ary transmitted signals $x_1, .., x_k$ in STBC which consists of two transmitters and two receivers, so the received signals are $y_{11}, .., y_{1n}, y_{12}, .., y_{qn}$.

The a-posteriori probabilities of the transmitted signals are computed according to Baye's rule as follows:

$$P(x_1,..,x_k|y_{11}..,y_{qn}) = P(y_{11}..,y_{qn}|x_1,..,x_k) * P(x_1,..,x_k) \quad (3.29)$$

where q represents the number of receivers, n represents the number of time slots needed to transmit each symbol and the conjugated symbol. $P(x_1,..,x_k)$ represents the a-priori information related to the transmitted symbols which can get them through the soft-decision feedback. Moreover, the conditional probabilities in Eq. (3.22) are computed over Rayleigh fading channel according to Bauch [36] as follows:

$$\mathrm{P}\big(y_{11}..,y_{qn}\big|x_1,..,x_k\big) = \frac{1}{(\sigma\sqrt{2\pi})^{qn}}\ exp\left\{-\frac{1}{2\,\sigma^2}\sum_{l=1}^{q}\sum_{i=1}^{n}\left|y_{l\,i}-\sum_{j=1}^{p}h_{l\,j}\,g_{j\,i}\right|^2\right\} \quad (3.30)$$

where g_{ji} represents all the elements of the transmission matrix in Eq. (3.7), sigma represents the variance of the noise. In addition, the a-posteriori probabilities for each transmitted signal x_i can be computed by simplifying Eq. (3.29) as follows:

$$P(x_i\mid y_{11}...,y_{qn}) = P(y_{11}...,y_{qn}|\,x_i)\ .\ P(x_i) \quad (3.31)$$

where $i = 1,..,k$ represents the constraint length of the coded symbols. The STBC used in this thesis relates to $p = 2, k = 2, n = 2$ according to the transmission matrix G_2 in Eq. (3.7). The computation of a-posteriori probabilities for k-ary transmitted signals in this STBC scheme can be done depending on Eq. (3.29) and Eq. (3.30) as follows [36]:

$$\begin{aligned} P(x_1,\dots,x_k\mid y_{11}\dots,y_{qn}) &= \\ &= C\,.\frac{1}{(\sigma\sqrt{2\pi})^{qn}}\exp\left\{-\frac{1}{2\,\sigma^2}\sum_{l=1}^{q}\left[\left|y_{l1}-\sum_{j=1}^{p}h_{l\,j}\,g_{j1}\right|^2+\left|y_{l\,2}-\sum_{j=1}^{p}h_{lj}\,g_{j2}\right|^2\right]\right\} \\ &= C'.exp\left\{-\frac{1}{2\,\sigma^2}\sum_{l=1}^{q}[\,|\,y_{l1}-h_{l1}\,g_{11}-h_{l\,2}\,g_{21}|^2+|\,y_{l2}-h_{l1}\,g_{12}-h_{l2}\,g_{22}|^2\,]\right\} \\ &= C'.exp\left\{-\frac{1}{2\,\sigma^2}\sum_{l=1}^{q}[\,|\,y_{l1}-h_{l1}\,x_1-h_{l\,2}\,x_2|^2+|\,y_{l2}-h_{l1}\,\bar{x}_2-h_{l2}\,\bar{x}_1|^2\,]\right\} \end{aligned} \quad (3.32)$$

where $C = P(x_1, \dots, x_k)$ represents a constant which means that there is no a-priori information (i.e. there is no iteration process at the receiver). Also $C' = C.1/(\sigma\sqrt{2\pi})^{qn}$ represents a constant. So, because of the orthogonality of codes, the computation of a-posteriori probabilities for each transmitted signal x_1 can be done by removing the related terms x_2 from Eq. (3.32) as follows:

$$P(x_1|\, y_{11} \dots, y_{q2}) = C'.exp\left\{-\frac{1}{2\,\sigma^2}\sum_{l=1}^{q}[\,|\,y_{l\,1} - h_{l\,1}\,x_1|^2 + |\,y_{l\,2} - h_{l\,2}\,\bar{x}_1|^2\,]\right\}$$

$$P(x_1|\, y_{11} \dots, y_{q2}) = C''.exp\left\{-\frac{1}{2\,\sigma^2}\sum_{l=1}^{q}[\,-h_{l1}\,x_1\bar{y}_{l1} - \bar{h}_{l\,1}\,\bar{x}_1\,y_{l1} - h_{l\,2}\,\bar{x}_1\,\bar{y}_{l2} - \right.$$

$$hl2\ x1\,yl2 + x12 i=12 hli2$$

(3.33)

where the transmitted signal x_1 does not depend on the terms $|y_{l1}|^2 and\ |y_{l2}|^2$ as seen in Eq. (3.33), so these terms are considered as constant and are merged with the other constant (C') in the equation to form new constant (C''). By following some simplification and shortcuts, Eq. (3.33) is simplified as follows:

$$P(x_1|y_{11} \dots, y_{q2}) = C''.exp\left\{-\frac{1}{2\,\sigma^2}\left[\left|\left[\sum_{l=1}^{q}(\,\bar{h}_{l\,1}\,y_{l1} + \bar{h}_{l\,2}\,\bar{y}_{l2})\right] - x_1\right|^2 + \right.\right.$$

$$-1 + l=1 q i=12 hli2\ x1$$

(3.34)

In the same manner, the computation of a-posteriori probabilities for each transmitted signal x_2 can be done by removing the related terms x_1 from Eq. (3.25) and by following some simplifications and shortcuts, Eq. (3.25) is simplified as follows:

$$P(x_1|y_{11} \dots, y_{q2}) = C''.\exp\left\{-\frac{1}{2\,\sigma^2}\left[\left|\left[\sum_{l=1}^{q}(\,\bar{h}_{l\,2}\,y_{l1} + \bar{h}_{l\,1}\,\bar{y}_{l2}\,)\right] - x_2\right|^2 + \right.\right.$$

$$-1 + l=1 q i=12\ hli2\ x2$$

(3.35)

3.7 Concatenated BICM-ID and STBC (BI-STC-ID)

The conception of space time block code (STBC) was explained in detail. The process of MAP decoding has been applied to STBC in section (3.6). By using this process, soft outputs are provided by the STBC. These soft outputs can be used as inputs to the following concatenated stage which may be one of the types of channel decoder. This means that STBC scheme can be concatenated with other types of channel codes to improve the system performance through achieving maximum coding gain in addition to the spatial gain over Rayleigh slow fading channel [20]. The increment of coding gain means increment in the transmission reliability by transmitting multiple copies of each symbol. The increment of spatial diversity means increment the transmission data rate. In this section, due to the coding gain provided by STBC is low, thus the BICM-ID scheme is concatenated with STBC depending on the availability of ideal channel estimator at the receiver to form a new enhanced BI-STC-ID scheme. The new BI-STC-ID scheme uses two types of interleaver, one of the types is the bit interleaver to interleave the bits at the output of convolutional encoder, and the other type is the symbol interleaver to interleave the symbols at the output of the demodulator. Furthermore, after the success in turbo codes, the new BI-STC-ID scheme contains on iterative decoding process at the receiver to mitigate the interference which may occur over the channel or through the receiver antennas.

3.7.1 System model

The communication system shown in Fig. 13 is a BI-STC-ID scheme with two transmitter antennas and two receiver antennas. This system consists of BICM-ID (bit interleaved coded modulation with iterative decoding) concatenated with STBC (space time block code) scheme [32, 37].

At the transmitter side shown in Fig. 13 (a), the random information bits are generated using the source information which are sent to the non-recursive convolutional encoder for encoding. The convolutional encoder consists of two inputs and three outputs (rate-2/3). The coded bits at the output of convolutional encoder are interleaved randomly using three independent S-random bit interleavers. The role of S-random interleavers has been described in section (2.4.2). The interleaved bits are grouped and sent to the 8-PSK modulator (Mapper) which uses a Gray mapping technique.

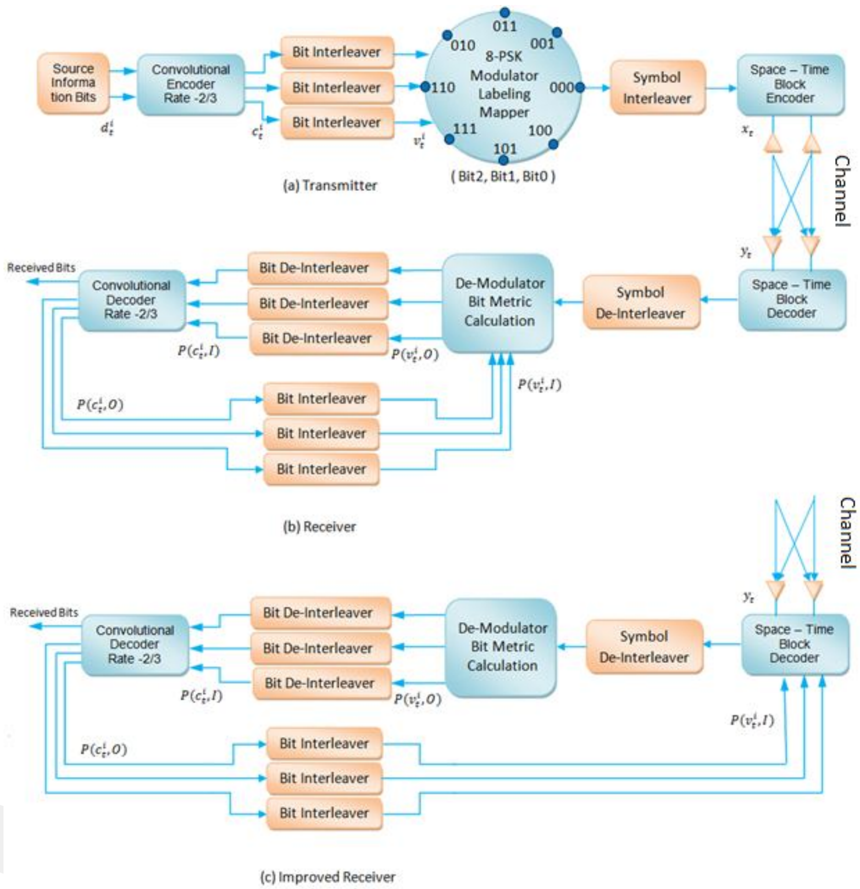

Figure 13 Communication system consisting of BICM concatenated with STBC with iterative decoding

The mapping process means that each three bits are assigned to one point (symbol) in the 8-PSK constellation which consists of $2^m = 2^3 = 8$ points (symbols). The symbols at the output of the 8-PSK modulator are interleaved using S-random symbol interleaver. Then the interleaved symbols are sent to the STBC encoder.

STBC encoder receives the interleaved symbols and divides them into two groups. The symbols in each group are encoded by generating the conjugated symbols. Two symbols are transmitted to the channel using two transmitter antennas simultaneously. Then the two conjugated symbols are transmitted to the channel in the next time slot [32, 37].

The transmitted symbols propagate over two independent fading channels to reach the receiver antennas. The fading amplitude for each channel has a variance 1. The fading amplitude for each channel is assumed constant during transmitting the symbols of each frame. The communication channels used in this thesis are AWGN and mobile channels.

At the receiver side shown in Fig. 13 (b), STBC decoder receives the transmitted signals using two antennas. The received signals are decoded by applying the MAP algorithm. The STBC decoder computes eight probabilities for each received signal representing the Euclidean distances between the received signal and all possible transmitted signals in the 8-PSK constellation [32, 37]. Then the computed probabilities for all received symbols are de-interleaved to restore their original sequence. The de-interleaved probabilities are sent to the 8-PSK demodulator. The 8-PSK demodulator computes six bit metrics for each received symbol depending on the eight probabilities. After that, all the bit metrics are de-interleaved using three bit de-interleavers and sent to the convolutional decoder as shown in Fig. 13 (b). The outer convolutional decoder depends on a simple Viterbi diagram to compute all the branch metrics between the previous state and the present state in each column of the Viterbi diagram. Finally, the convolutional decoder computes all the forward and backward probabilities and all max likelihood metrics for each received symbol to make the hard decision to restore the transmitted information bits and to compute the soft values to return the feedback information in each iteration process.

The iteration process is an execution of the demodulation and decoding processes at the receiver several times to overcome the interference and improve system performance by reducing the bit error rate. The iteration process is executed by returning the feedbacks from the output of the convolutional decoder to the input of the demodulator after interleaving operation as shown in Fig. 13 (b). These feedbacks are used to compute the a-priori probabilities for all received symbols at the modulator.

In an attempt to develop system performance, we proposed a new method to execute the iteration process by re-turning the feedbacks from the output of the convolutional decoder to the input of STBC decoder instead of re-turning the feedbacks to the input of the demodulator as shown in Fig. 13 (c). As a result of using this new method for iteration process in BI-STC-ID scheme, the system performance has been improved with 0.5 dB as indicated in Chapter-5.

3.8 Wireless Channel Models

In wireless systems, the most important things to understand the characteristics of the available wireless channels are the design of link budget between the transmitter and the receiver, the design of transmission protocol, and the design of coherent receiver. The behavior of the wireless channels is random and unreliable because of the quick changes in the channels' status in a too short time leads to make the communication over these channels a difficult task.

The wireless channels are classified into different types which can discriminate between them by the environment of propagation. There are many environments of propagation such as suburban, orbital, urban, underwater, and indoor [38, 39].

The performance of the wireless systems is limited because of the impact of various characteristics of the wireless channel. The wireless channel between the transmitter and the receiver (transmission data path) may be a simple path like line-of-sight or may be a path that contains on many obstructions like mountains, towers, buildings and foliage. Also among the other factors that affect the signal transmitted over the wireless channel is the speed of mobile unit. The speed of mobile unit affects the speed of fading signal level. The design of any wireless communication system requires the knowledge of the wireless channel modeling which is usually done using a statistical method. The statistical methods depend mainly on the practical measurements which were conducted for a particular communication system.

The propagation of electromagnetic waves over the wireless channel is attributed to many mechanisms but generally they can be limited to the reflection, the scattering and the diffraction as illustrated in Fig. 14. The reflection happens when the electromagnetic waves fall on a surface with dimensions much larger than the wavelength of the signals. The scattering happens when the wavelength of the electromagnetic signals equal or much larger than the dimensions of the object that fall on it as well as its irregular shape which cause to redirect the direction of the transmitted energy into many directions. Diffraction happens when there is a large object blocking the direct path between the transmitter antenna and the receiver antenna which causes to generate secondary waves in the back of the obstructive object.

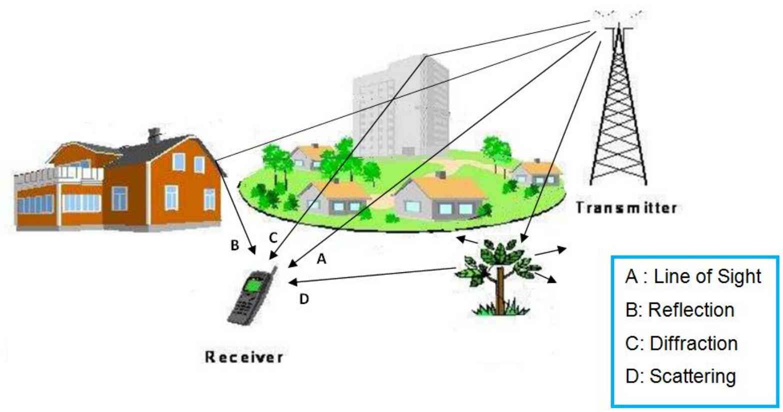

Figure 14 Propagation of electromagnetic waves over the wireless channel

The propagation of radio waves can be described approximately by the independent phenomena shadowing, path loss, and fading. Each phenomenon resulting from the principle of latent physicist. Each phenomenon should be taken into account when designing and evaluating the wireless systems [38, 39]. The path loss has a deterministic and known effect. And this effect is inversely proportional to the distance between the transmitter and the receiver. On the contrary, shadowing and fading phenomena don't have a deterministic effect which means the effect of these phenomena changes randomly. The shadowing phenomenon happens because of presence the different shapes of terrain and the large buildings which stand between the main station and the mobile unit and preventing the line-of-sight between them.

The fading phenomenon causes large changes in the attenuation during small periods of time like microseconds, where this phenomenon occurs always as a result of the multipath propagation environment. The transmitted electromagnetic waves which pass through the multipath propagation environment are reflected several times causing to generate multi-copies of the same wave which interfere with each other at the receiver antenna.

In wireless systems, fading phenomenon is usually represented using the Rayleigh distribution model. The Rayleigh fading model is described using the autocorrelation function and the power spectral density function. The autocorrelation function relates to the motion of the receiver and the transmitter which in turn depends on Doppler frequency [38, 39].

AWGN model is a transmission channel in many wireless systems. The AWGN channel model is described as a poor model in practice. The channel model the most frequent in practice is the fading channel. The fading channel is a non Gaussian channel characterized with the precision and complexity. The mobile channel is a powerful example of fading channel, where the radio waves are reflected several times to compose multiple paths for the transmitted waves. There are two conceptions of the fading large-scale and small-scale.

3.8.1 Large-scale fading

Large-scale fading is a type of fading on the transmitted signal value defined as the path loss or the average attenuation value of the signal because of the motion of the signal to longer distances. The fading in the signal value depends on the position of the mobile unit, the distance between the mobile unit and the transmitter, the type of antenna used, etc. The fading in the signal value may also depend on the existence of large and high terrain and objects in the arriving path to the receiver which leads to the shadowing phenomenon. This type of fading can be noticed after long distances from the transmitter (equal several tens of wavelength of the carrier signal).

3.8.2 Small-scale fading

This type of fading occurs due to the large changes in the amplitude and the phase of the transmitted signal, where the transmitted signal reaches the receiver from multiple paths due to the reflected, diffracted and scattered waves from many obstructions. The signal in each path has a different amplitude and phase. The combined signal at the receiver antenna has different values that change randomly.

If the number of signal paths is large and there is no a line-of-sight path between the transmitter and the receiver, thus the combined signal at the receiver has an envelope which is described statistically as a Rayleigh PDF as shown in Fig. 15. On the other hand, if there is a line-of-sight path between the transmitter and the receiver, thus the combined signal at the receiver has an envelope which is described statistically as a Rician PDF [38, 39].

In wireless systems, several models were suggested to simulate the Rayleigh fading channel. These models are either deterministic or statistical. The deterministic models perform approximate processes for the Gaussian random operations by combining a finite number of sinusoids which are selected properly. The statistical models compute the densities of power spectral related to the white Gaussian random operations using the filtering in frequency-domain or time-domain. For instance, the deterministic models are Clarke model (Clarke 1968) [40] and Jakes model (Jakes 1974) [41], while the statistical models are Inverse Discrete Fourier Transform (IDFT) (Smith 1975) [42] and White Noise Filtering (Omidi 1999) [43].

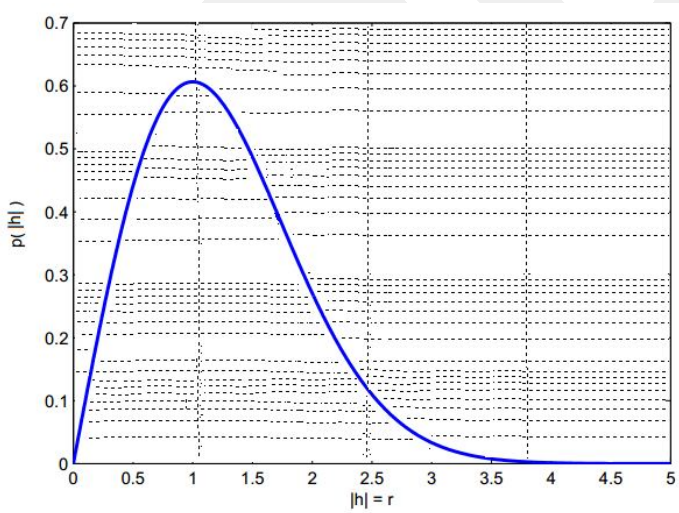

Figure 15 Probability density function of the envelope of Rayleigh fading channel

3.8.3 Deterministic model of sum of sinusoids

The wireless fading channel has a complex envelope which can be represented by combining several components of homogeneous waves. Each component of the homogeneous waves is a sinusoidal wave with specific values of the frequency, amplitude and phase. Thus, the waveform of the fading channel is represented mathematically by summing several sinusoidal waves. This representation of the fading channel is "sum of sinusoids". Many models were presented depend on the sum of sinusoids to simulate the fading channel such as Clarke's model (Clarke 1968).

The reference model Clarke (Clarke 1968) [40] can be represented in mathematical expression to define the complex gain of the fading channel under the following assumptions non-selective frequency fading channel (flat fading) and non-dominant path (non line of sight) as follows:

$$h(t) = \sqrt{\frac{2}{N}} \sum_{n=1}^{N} e^{j\,[2\pi f_d t \cos(\alpha_n) + \emptyset_n]} \tag{3.36}$$

where f_d represents the maximum value of Doppler frequency, N represents the total number of multipath components, $\alpha_n \sim U[-\pi,\pi]$ represents the value of the arrival angle to the receiver, and $\emptyset_n \sim U[-\pi,\pi]$ represents the random value of the phase. The efficiency of the Clarke's model is low because there are many random variables. So, another model of the sum of sinusoids was proposed by Jake (Jakes 1974) [41] to simulate the fading channel using the following mathematical expressions:

$$\begin{aligned} h_I(t) &= \sqrt{2}\cos(2\pi f_d t)\,.\,2\sum_{n=1}^{M} \cos\left(\frac{2\pi n}{M}\right)\cos\left(2\pi f_d \cos\left[\frac{2\pi n}{4M+2}\right]t\right) \\ h_Q(t) &= 2\sum_{n=1}^{M} \sin\left(\frac{2\pi n}{M}\right)\cos\left(2\pi f_d \cos\left[\frac{2\pi n}{4M+2}\right]t\right) \end{aligned} \tag{3.37}$$

where M represents the total and the finite number of sinusoids, $h_I(t)$ represents the in-phase (real) component, $h_Q(t)$ represents the quadrature-phase (imaginary) component. Jake’s model was the widely used model because it reduced the number of sinusoids in the model by taking advantage of the presence of the symmetry in the environment. For example, the values of arrival angles are distributed over the range $(-\pi,\pi)$ in Clarke's model which lead to positive and negative values for Doppler frequencies but Jake's model take only the positive values of the Doppler frequencies to decrease the number of the sinusoids.

The recent researches (Beaulieu & Young 2001) [44] and (Xiao & Zheng 2002) [45] proved that the envelope of the fading channel simulated by Jake's model is identical in each execution process because the parameters of the model does not change in each execution process.

Xiao and Zheng (Zheng & Xiao 2002) [45] suggested new statistical methods to simulate the fading channel. Each method uses different parameters in the simulation model which change in each execution process. In this thesis, one of the statistical methods is adopted as a special model of the fading channel for the wireless system BI-STC-ID. This statistical method uses a specific number of sinusoidal waves to simulate the fading channel efficiently. The mathematical expressions used in this method to simulate the envelope of the Rayleigh fading channel are as follows:

$$h[n] = h_I[n] + jh_Q[n],$$
$$h_I[n] = \frac{1}{\sqrt{N_s}} \sum_{k=1}^{N_s} \cos(B_n)\ cos(2\pi f_d \cos\alpha_k + \emptyset_k)$$
$$h_Q[n] = \frac{1}{\sqrt{N_s}} \sum_{k=1}^{N_s} \sin(B_n)\ \sin(2\pi f_d\, cos\,\alpha_k + \varphi_k)$$
$$\alpha_k = \frac{\pi k - 0.5\,\pi}{2N_s},\quad B_n = \frac{k\pi}{N_s},\quad \emptyset_k = \varphi_k \frac{2\pi\ random(N_s)}{N_s},$$
$$f_d = f.\frac{s}{C},\ k = 1,2,\ldots,N_s \tag{3.38}$$

Where φ_k and $\emptyset_k$ are distributed uniformly over $(-\pi,\pi)$ and they are changed randomly and independently in a statistical manner for all values of k, N_s represents the finite number of the sinusoidal waves, f_d represents Doppler frequency shift, f represent the frequency of the carrier signal, s represents the speed of the mobile unit, $C = 3.10^{-8}$ represent speed of the light.

In this thesis, we used the following parameters for our wireless channels, $f = 1800\ MHz$ the frequency of the carrier signal, $s = 30\ km/h$ the speed of the mobile unit, $N_s = 8$ the finite number of the sinusoidal waves. Also, we assumed that each value of the envelope of the fading channels remains constant for all symbols of the frame.

CHAPTER 4

COOPERATIVE COMMUNICATION SYSTEMS

4.1 Introduction

The performance of communication systems over fading and AWGN channels is improved using many techniques. As mentioned in Chapter-2, BICM-ID scheme proposed by Zehavi [10] improves the performance over AWGN and fading channels using the bit interleaver and the simple iterative decoding respectively.
BI-STC-ID [14] scheme was proposed by Li and Ritcey for data transmission from a single transmitter to a single receiver as mentioned in Chapter-3. The BICM-ID scheme is concatenated with STBC to increase the system performance over different conditions of the fading channels. The STBC provides spatial diversity and coding gain using multiple antennas at the transmitter and the receiver (MIMO) which lead to increase the area coverage and the data rate without the need to increase the bandwidth and the transmitted power. However, the spatial diversity is limited only on the transmitter side because the small size of the mobile receiver unit which creates several challenges concerning with the power consumption and the complexity. In this chapter, a recent technique suggested by Nosratinia [46] called the cooperative diversity is applied on BI-STC-ID scheme to address the problems to get enormous potential for the next generations of wireless communication networks. The use of cooperative technique distributes several intermediate stations (relays) between the source and the destination in different paths to get the cooperative communications as shown in Fig. 16. This technique makes the whole system more reliable with respect to the throughput and the bit error rate (BER).

The use of cooperative communications convert the BI-STC-ID communication system consists of a single source and a single destination to the communication system consists of multiple sources and multiple destinations (virtual MIMO). In the cooperative systems, multiple copies of the signals are transmitted from the source to one or more secondary stations (relays) and to the destination simultaneously. Each secondary station (relay) receives, decodes, re-encodes and re-transmits the signals to the destination. At the destination multiple copies of the signals from the source and the relays are received in different time slots and then they are combined together using several techniques of combination to extract the transmitted original symbols from the source [46, 47].

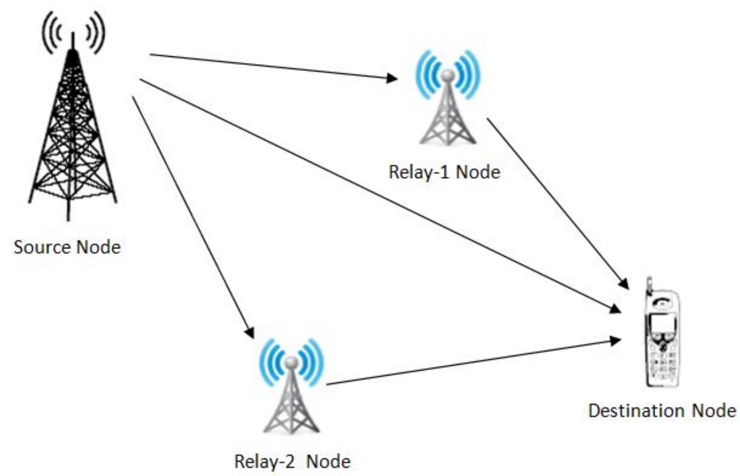

Figure 16 Cooperative communication system using two relay nodes

In the cooperative systems, two types of cooperative protocols are used in the secondary stations (relays) to overcome the effects of multipath fading channel decode-and-forward protocol (DF) and amplify-and-forward protocol (AF). Each protocol has certain abilities under different conditions of the channel. In the cooperative systems which use the DF protocol, each relay node receives the signals from the source node, decodes, re-encodes and retransmits them to the destination node. In the cooperative systems which use the AF protocol, each relay node receives the signals from the source, amplifies, and retransmits them to the destination. Both cooperative protocols match well with the coding rates and with the highest order of modulation (such as 8-PSK, 16-QAM) used in the source and relay nodes. To increase the throughput of the cooperative systems, the source and relay nodes firstly check the reliability of the wireless channels' condition between the source, relay and destination nodes and then they increase their modulation order [47, 48].

4.2 Cooperative System Model

An example of the cooperative BI-STC-ID-DF scheme is shown in Fig. 17. This cooperative system consists of a single source, two relays and single destination. The source and relay nodes are assumed have the same transmitter module mentioned in Chapter-3 which consists of convolutional encoder with rate-2/3, 8-psk modulator, and STC encoder with two antennas. The destination and relay nodes are assumed to have the same receiver module mentioned in Chapter-3 which consists of STC decoder with two antennas, 8-psk demodulator, and convolutional decoder. The iteration process is formed by returning the feedback from the convolutional decoder to the STC decoder. The cooperative protocol used in each relay node is DF which means that each relay receives the signals, decodes, re-encodes and re-transmits them again to the destination [47, 48]. The wireless fading channels between any two nodes in the cooperative system, source, relay and destination are Rayleigh fading channels and they are assumed independent from each other randomly. The coefficients of the fading channels are distributed randomly and independently in a Gaussian manner with variance equals $N_\circ/2$ and mean equals zero.

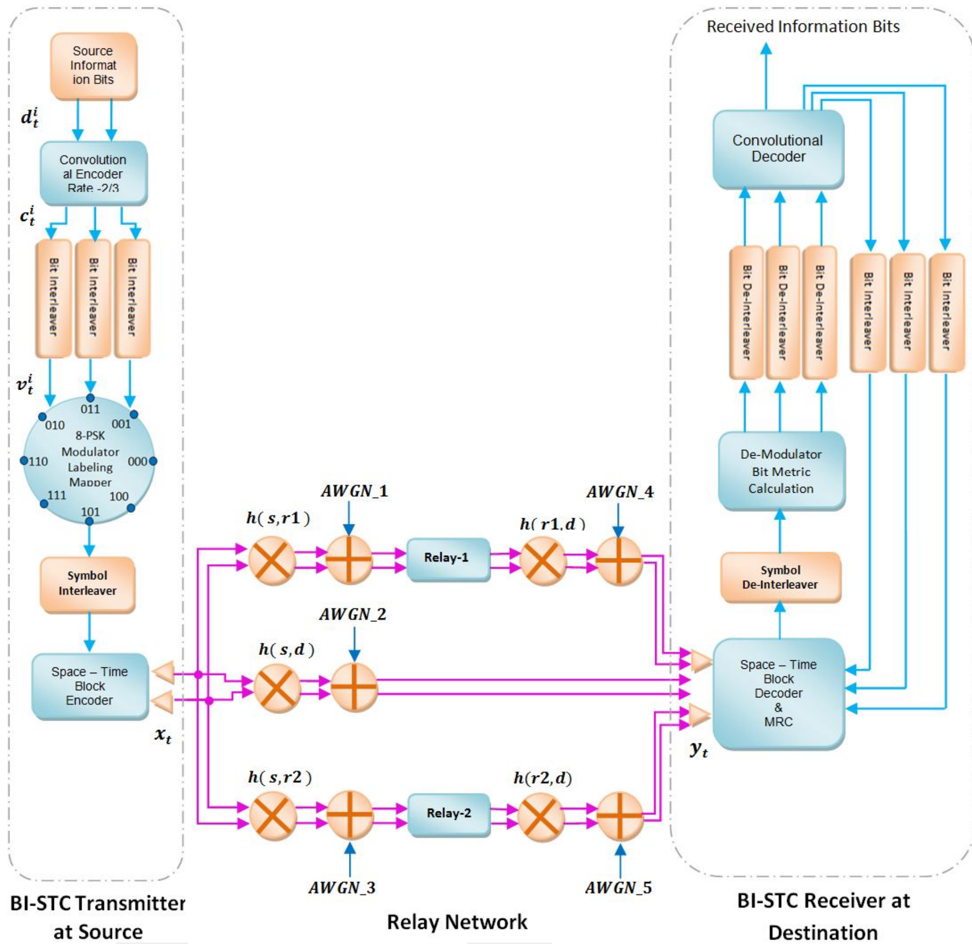

Figure 17 Cooperative BI-STC-ID-DF consists of single source, two relays and single destination

The process of transmitting each frame is conducted in two phases. The first phase is conducted in the source node. The second phase is conducted in the relay nodes.

4.2.1 Source node

The source node is considered the first phase of transmitting each frame. The information bits are encoded firstly using the convolutional encoder with rate-2/3. The coded bits at the output of the encoder are interleaved using three bit interleavers. Three interleaved bits are grouped together at the same time slot using 8-psk modulator and converted to complex symbol. The symbols are interleaved using symbol interleaver and sent to the STC encoder. The interleaved symbols are encoded again using the STC encoder. Each two symbols are transmitted together at a certain time slot by two antennas, where each symbol is transmitted by one antenna over different fading channel. The frames are broadcasted from the source to the destination and relay nodes over different fading channels simultaneously [47, 48].

4.2.2 Relay node

The cooperative protocol used at each relay node is decode-and-forward (DF) which means that the relay node decodes the received signals, re-encodes, re-transmits them again. The received signals at each relay node from the source node are decoded correctly by receiving two signals at a certain time slot and then receiving their conjugated signals at the next time slot using two antennas as follows:

$$y_{i1}(s,r_j) = \sqrt{p}\,[\,h_{i1}(s,r_j)\,x_1(s,r_j) + h_{i2}(s,r_j)\,x_2(s,r_j) + n_{i1}(s,r_j) \qquad (4.1)$$

$$y_{i2}(s,r_j) = \sqrt{p}\,[\,h_{i1}(s,r_j)\,\bar{x}_2(s,r_j) + h_{i2}(s,r_j)\,\bar{x}_1(s,r_j) + n_{i2}(s,r_j) \qquad (4.2)$$

where $i \in \{1, 2\}$ represents the antenna's sequence, $j \in \{1, 2\}$ represents the relay's sequence and p represents the transmitted power from the source. The received signals are decoded by applying the MAP algorithm in the STBC decoder as mentioned in section (3.6). The a-posteriori probabilities produced from the STBC decoder are de-interleaved and sent to the demodulator. The bit metrics produced from the demodulator are sent to the convolutional decoder to restore the transmitted information bits and compute the feedback for the iteration process.

The second phase of transmitting each frame is conducted at the relay nodes, where after restoring the original information bits at each relay node, each relay node re-encodes and re-transmits the original information bits again to the destination. Using the same transmitter model at the source node, two symbols are transmitted together at a certain time slot from each relay by two antennas. The transmitted symbols from each relay node hold the same sequence of the original information bits transmitted from the source node but with different representations of the symbols [47, 48].

4.2.3 Destination node

The destination node is considered the phase of receiving all the symbols transmitted from the source and relay nodes. In the cooperative systems, the destination node receives four signals from each node (source and relays) at different time slots by two antennas as follows:

From the source node

$$y_{i1}(s,d) = \sqrt{p}\,[h_{i1}(s,d)x_1(s,d) + h_{i2}(s,d)x_2(s,d) + n_{i1}(s,d)] \quad (4.3)$$

$$y_{i2}(s,d) = \sqrt{p}\,[h_{i1}(s,d)\bar{x}_2(s,d) + h_{i2}(s,d)\bar{x}_1(s,d) + n_{i2}(s,d)] \quad (4.4)$$

From the relay-1 node

$$y_{i1}(r_1,d) = \sqrt{p_1}\,[\,h_{i1}(r_1,d)\,x_1(r_1,d) + h_{i2}(r_1,d)\,x_2(r_1,d) + n_{i1}(r_1,d)] \quad (4.5)$$

$$y_{i2}(r_1,d) = \sqrt{p_1}\,[\,h_{i1}(r_1,d)\,\bar{x}_2(r_1,d) + h_{i2}(r_1,d)\,\bar{x}_1(r_1,d) + n_{i2}(r_1,d)] \quad (4.6)$$

From the relay-2 node

$$y_{i1}(r_2,d) = \sqrt{p_2}\,[\,h_{i1}(r_2,d)x_1(r_2,d) + h_{i2}(r_2,d)x_2(r_2,d) + n_{i1}(r_2,d)] \quad (4.7)$$

$$y_{i2}(r_2,d) = \sqrt{p_2}\,[\,h_{i1}(r_2,d)\bar{x}_2(r_2,d) + h_{i2}(r_2,d)\bar{x}_1(r_2,d) + n_{i2}(r_2,d)] \quad (4.8)$$

where Eq. (4.3) & Eq. (4.4) represent the received signals at the destination node from the source node, Eq. (4.5) & Eq. (4.6) represent the received signals at the destination node from the relay-1 node, Eq. (4.7) & Eq. (4.8) represent the received signals at the destination node from the relay-2 node, $i \in \{1,2\}$ represents the antenna's sequence, $j \in \{1,2\}$ represents the relay's sequence, p represents the transmitted power from the source node, p_1 represents the transmitted power from the relay-1 node, p_2 represents the transmitted power from the relay-2 node [47, 48].

All the received signals at the destination node are combined using different techniques of the combination to get better extraction of the transmitted original symbols from the source node to improve the system performance. One of these techniques is a product of the sum of all the received signals to get the total received signals as follows:

$$y_{i1}(d) = y_{i1}(s,d) + y_{i1}(r_1,d) + y_{i1}(r_2,d) \quad (4.9)$$

$$y_{i2}(d) = y_{i2}(s,d) + y_{i2}(r_1,d) + y_{i2}(r_2,d) \quad (4.10)$$

These final received signals are decoded by applying the MAP algorithm in the STBC decoder and generating a-posteriori probabilities for each final signal as mentioned in section (3.6).

Another technique to combine all the received signals at the destination node is a product of the sum of all the computed a-posteriori probabilities for the received signals from each node. The received signals at the destination node from the source, relay-1 and the relay-2 nodes are decoded separately by applying the MAP algorithm in the STBC decoder and generating a-posteriori probabilities for each node. The total a-posteriori probabilities are as follows:

$$1- \; Ps(d) = [\,Ps(s,d) + Ps(r_1,d) + P(r_2,d)]/3$$

$$2- \; Ps(d) = [\,0.8\,Ps(s,d) + 0.2\,Ps(r_1,d) + 0.2\,P(r_2,d)]/3$$

where $Ps(s,d) > Ps(r_1,d)$ & $Ps(r_2,d)$ OR

$$Ps(d) = [0.2\,Ps(s,d) + 0.8\,Ps(r_1,d) + 0.2\,P(r_2,d)]/3$$

where $Ps(r_1,d) > Ps(s,d)$ & $Ps(r_2,d)$

$$3- \; Ps(d) = [Ps(s,d) + 0.1\,Ps(r_1,d) + 0.1\,P(r_2,d)]/3$$

$$4- \; Ps(d) = [Ps(s,d) + 0.2\,Ps(r_1,d) + 0.2\,P(r_2,d)]/3 \quad (4.11)$$

where $Ps(s,d)$ represents the generated a-posteriori probabilities for the received signals from the source node at a certain time slot, $Ps(r_1,d)$ represents the generated a-posteriori probabilities for the received signals from the relay-1 node at a certain time slot and $Ps(r_2,d)$ represents the generated a-posteriori probabilities for the received signals from the relay-2 node at a certain time slot. All the generated a-posteriori probabilities for all the received symbols are de-interleaved using the symbol de-interleaver and sent to the demodulator to generate the bit metrics for all the received symbols. All the generated bit metrics are de-interleaved using the bit de-interleavers and sent to the convolutional decoder. The convolutional decoder depends on the bit metrics to generate four types of probabilities branch metrics, forward metrics, backward metrics and max likelihood metrics for each received symbol. The generated four probabilities are used to make the hard decision to restore the original information bits and compute the feedback metrics for the iteration process [47, 48].

The performance of the cooperative BI-STC-ID-DF system is illustrated in Chapter-5 for different techniques of the combination used at the destination node. We assumed the same power are transmitted from all the antennas at the source and relay nodes.

CHAPTER 5

SIMULATION RESULTS

5.1 Introduction

The mechanism of action of BICM-ID, BI-STC-ID and BI-STC-ID-DF schemes are described and discussed in Chapter-2, Chapter-3 and Chapter-4 respectively. In this chapter, these schemes have been simulated using C++ programming, where the simulation results have been provided to describe the performance of these schemes over AWGN and mobile fading channels.

From the simulation results below, we noticed the BICM-ID scheme has a good performance over AWGN channel. The performance of BICM-ID scheme over Rayleigh fading channel is improved by concatenating BICM-ID scheme with STBC to meet the growing demand on the wide bandwidth over mobile networks. The STC provides spatial diversity and coding gain to improve the system performance for high data rate. The small size of the mobile unit leads to create several challenges concerning with the power consumption and the complexity. The BI-STC-ID scheme is improved using intermediate stations (relays) between the transmitter and the receiver. All the wireless communication systems used in this thesis have an input block of information bits equals 2048 bits. These systems use Gray mapping at the 8-PSK modulator. The interleaver significantly affects the performance of the wireless systems therefore two types of interleavers are used in these systems bit interleaver and symbol interleaver. The different sequences of S-random interleavers are designed in this thesis with length and depth equal 1024, 15 respectively according to the rules mentioned in section (2.4.2). The wireless channels supported in this thesis are AWGN and mobile channels that have been simulated using C++ programming according to the sophisticated Jake's model mentioned in section (4.2). The mobile channel is a Rayleigh fading channel with multiple paths between the transmitter and the receiver and with the effect of Doppler frequency shift due to the motion of the receiver or the transmitter. In the multiple-inputs multiple-outputs (MIMO) systems, it is possible to assume there is a virtual fading channel between each transmitter antenna and each receiver antenna. All the coefficients of the fading channels are assumed constant during transmitting all the symbols of each frame. The speed of the receiver and the carrier signal frequency have been imposed to be 30 km/h and 1800 MHz respectively.

5.2 Simulation Results of BICM-ID Scheme

The structure of the BICM-ID scheme has been simulated using C++ programming. The simulation results have been sketched on form BER vs. SNR curve to describe the system performance over the AWGN and mobile fading channels. The BICM-ID system is illustrated in Fig. 8. The transmitter module consists of non-recursive convolutional encoder with rate-2/3, three independent bit interleavers and 8-PSK modulator with Gray mapping. The receiver module consists of 8-PSK demodulator, three bit de-interleavers and MAP decoder. The MAP decoder computes two types of the a-posteriori probabilities to generate the feedback and make the decision to recover the information bits. The demodulation and decoding processes are iterated several times using the generated feedback. The performance of the coded modulation TCM and BICM schemes have been sketched for comparison.

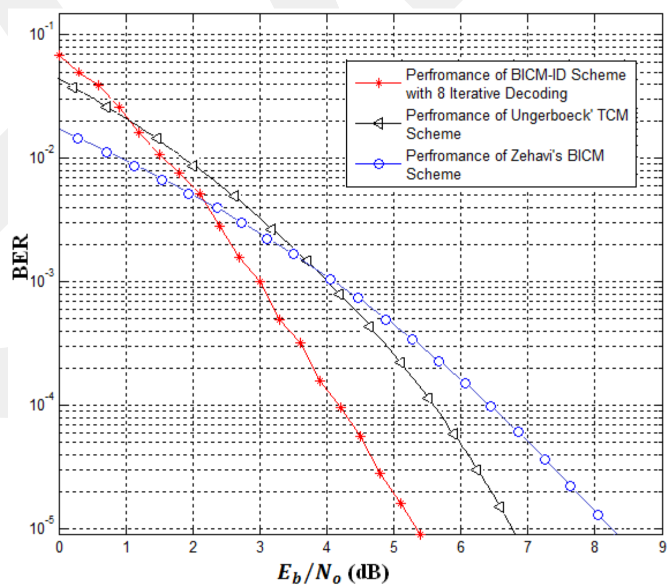

Figure 18 Performance of the BICM-ID scheme over AWGN channel with 8-state and 2048 information bits/block

The BICM-ID performance over the AWGN channel is represented at the receiver by sketching the BER vs. SNR curve as shown in Fig. 18. The BICM-ID performance has been improved with $1.5\ dB$ when $BER = 10^{-5}$ comparing with the performance of the TCM and BICM schemes over the AWGN channel. The BICM-ID performance over the mobile fading channel is represented at the receiver by sketching the BER vs. SNR curve as shown in Fig. 19.

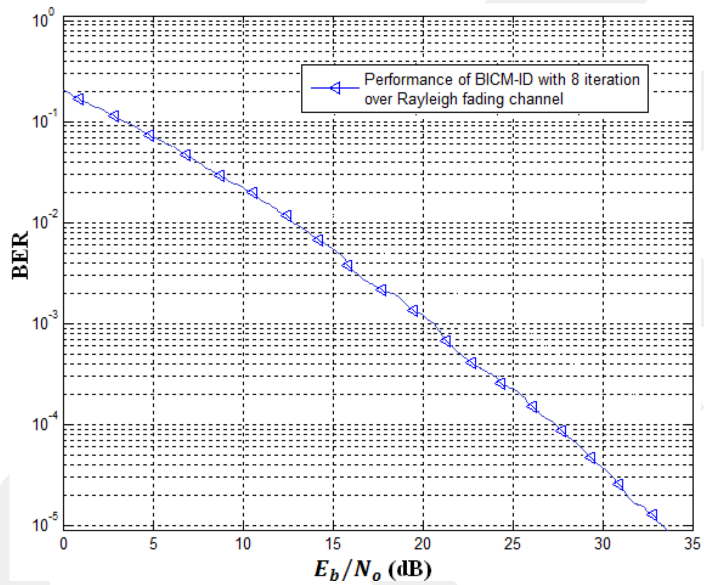

Figure 19 Performance of the BICM-ID scheme over mobile fading channel with 8-state and 2048 information bits/block

5.3 Simulation Results of BI-STC-ID Scheme

The structure of the BI-STC-ID scheme has been simulated using C++ programming. The simulation results have been sketched on form BER vs. SNR curve to describe the system performance over the mobile fading channel. The BI-STC-ID system is illustrated in Fig. 13. This system consists of BICM-ID scheme concatenated with STBC to increase the reliability of data transmission and the data rate by increasing the coding gain and the spatial diversity of the system respectively. The use of MAP algorithm in the STBC decoder facilitates the connection between the STBC with BICM-ID scheme, where the soft outputs of the MAP algorithm are used as inputs to the BICM-ID decoder. The transmitter module consists of non-recursive convolutional with rate-2/3, three independent S-random bit interleavers, 8-PSK modulator with Gray mapping, symbol interleaver and STBC encoder with two antennas. The receiver module consists of STBC decoder with two antennas, symbol de-interleaver, 8-PSK demodulator, three bit de-interleavers and MAP decoder. The MAP decoder computes two types of the a-posteriori probabilities to generate the feedback and make the decision to recover the information bits. The performance of BI-STC-ID scheme over mobile fading channel is represented at the receiver by sketching the BER vs. SNR curve as shown in Fig. 20. The BI-STC-ID performance has been improved more than $15\,dB$ when $BER = 10^{-5}$ comparing with the performance of the BICM-ID scheme shown in Fig. 19 over the mobile channel. Also The BI-STC-ID performance has been improved with 0.5 dB when $BER = 10^{-5}$ by when conducting a new feedback connection between the MAP decoder and the STBC decoder rather than the previous feedback connection between the MAP decoder and the demodulator.

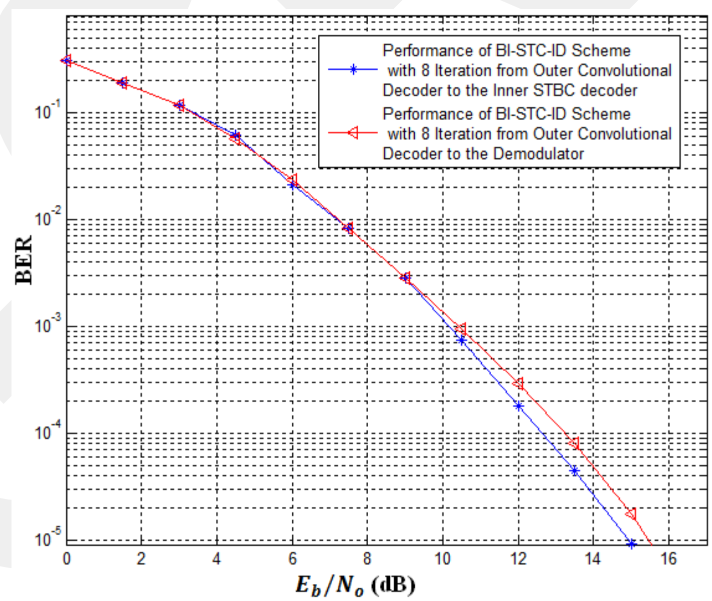

Figure 20 Performance of the BI-STC scheme over Mobile fading channel with 8-state and 2048 information bits/block

5.4 Simulation Results of BI-STC-ID-DF Scheme

The structure of the BI-STC-ID-DF scheme has been simulated using C++ programming. The simulation results have been sketched on form BER vs. SNR curve to describe the system performance over the mobile fading channel. The BI-STC-ID-DF system is illustrated in Fig. 17. The structure of this system is similar to the structure of BI-STC-ID system in section (5.3) with adding two secondary stations (relays) between the source and the destination to improve the performance by increasing its cooperative diversity. However, this cooperative system consists of single source node, two relay nodes and single destination node. The source and relay nodes have the same transmitter module's structure for the BI-STC-ID scheme. The transmitter module consists of convolutional encoder with rate-2/3, three bit interleavers, 8-psk modulator, symbol interleaver and STC encoder with two antennas. The destination and relay nodes have the same receiver module's structure for the BI-STC-ID scheme. The receiver module consists of STC decoder with two antennas, symbol de-interleaver, 8-psk demodulator, three bit de-interleavers and MAP decoder. The cooperative protocol used in each relay node is a decode-and-forward (DF). Each relay node receives the signals from the source node, decodes, re-encodes the information bits again and re-transmits them again to the destination. At the destination node multiple copies of the transmitted symbols are received from the source and relay nodes in different time slots. These copies are combined using several techniques of the combination to extract the transmitted original symbols from the source node. The BI-STC-ID-DF performance over mobile fading channel is represented at the receiver by sketching the BER vs. SNR curve as shown in Fig. 21 and Fig. 22. The BI-STC-ID-DF performance has been improved when $BER = 10^{-5}$ comparing with the performance of the BI-STC-ID scheme shown in Fig. 20 using several techniques of the signals combination at the receiver node.

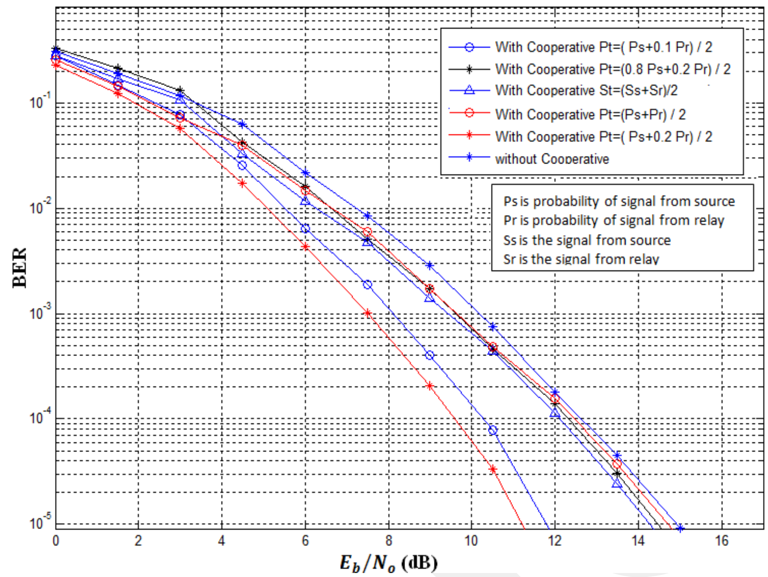

Figure 21 Performance of the BI-STC-ID-DF scheme with one-relay over mobile fading channel using different techniques of signal combination at the receiver node

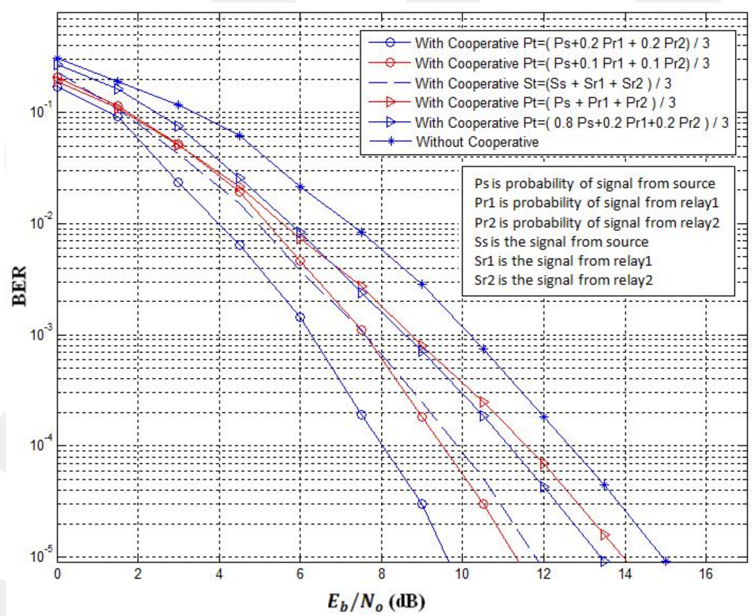

Figure 22 Performance of the BI-STC-ID-DF scheme with two-relays over mobile fading channel using different techniques of signal combination at the receiver node

CHAPTER 6

CONCULUSION

The simulation results demonstrated that the performance of wireless communication systems can be improved using different coding techniques without the need to increase the transmitted power or data rate. Extra copies of the symbols are transmitted for correcting the errors and decreasing the bit error rate. The simulation results showed the performance of BICM-ID scheme proposed by Li and Ritcey is better over the AWGN and Rayleigh fading channels than the performance of the traditional schemes such as TCM and BICM limited over the AWGN channel. Also the simulation results demonstrated that the performance of BICM-ID scheme is approximately identical to the performance of the turbo code scheme proposed by Berrou [28] but with low complexity. The ideal design of S-random interleaver, signals mapping and iterative decoding in BICM-ID scheme leads to get a maximum diversity. Also the simulation results demonstrated that this communication system has a coherent and appropriate performance over the AWGN and Rayleigh fading channels.

The use of multiple antennas at the transmitter or receiver units or both (MIMO) leads to increase the data rate and the reliability of the received data at the receiver through increasing the spatial diversity and the coding gain respectively. The small size of the mobile receiver unit makes the use of multiple antennas limited only on the base stations because of the limitation in the power consumption and the complexity. The coded modulation schemes like BICM-ID can concatenate with the STBC in series to form a more coherent BI-STC-ID scheme. The BI-STC-ID scheme improves the performance through merging the techniques which give the different diversities like 8-PSK modulator, interleaver, multiple antennas and iteration process. The receiver has perfect information about the channel coefficients by assuming it has a channel estimator. The iteration process is executed in two ways, the first way by making the feedback connection between the convolutional decoder and the demodulator, while the second way by making the feedback connection between the convolutional decoder and the STBC decoder. The second way of the feedback connection leads to improve the system performance greater than the first way as shown in the simulation results. There is a virtual fading channel between each transmitter antenna and each receiver antenna. Each virtual fading channel is a multi-paths channel and the coefficients of its envelope can be imposed fixed practically during transmitting all the symbols of each frame and changed from frame to another.

The probability of arrival of the transmitted signals to the receiver can be increased properly using secondary stations (relays) between the transmitter and the receiver to improve the system performance. It is obvious from the simulation results for the cooperative BI-STC-ID-DF system uses two transmitter and receiver antennas that there is improvement in the performance compared with the performance of the same communication system without using relay nodes. The transmitted signals by the two antennas of the source node (transmitter) are received by the two antennas of the destination node (receiver) and the two antennas of the relay nodes in different time slots. The received signals at each relay node are decoded, re-encoded, and then re-transmitted again to the destination node. All the received signals at the destination node from the source and the relay nodes are combined together using different several techniques of the signals combination to increase the probability of restoring the transmitted information bits properly. For the linear combination of the signal probabilities received from source and relays, it is seen that proper decision of the coefficients used during linear combination is an important criteria for the performance of cooperated communication systems.

One of the future works can be the integration of the BI-STC-ID-ID system with the OFDM system to increase the transmitting data rate per user and to make the received data more reliable over mobile fading channel. Another future work may be the control on the relays' signals at the destination node and choosing the best signals and then applying the different combination techniques on them.

REFERENCES

1. **Streele R., Hanzo L., (1999),** "*Mobile Radio Communications: Second and Third Generation Cellular and WATM Systems*", New York, pp. 757-761.

2. **Wachsmann U., Huber J., (1995),** "*Power and Bandwidth Efficient Digital Communication Using Turbo Codes in Multilevel Codes*", European Transaction on Telecommunications (ETT), vol. 6 pp. 557.

3. **Parsons D., (1992),** *"The Mobile Radio Propagation Channel"*, Pentech Press, London, pp. 217-219.

4. **Gesbert D., Shafi M., Shiu D. S., (2003),** *"An Overview of MIMO Space-Time Coded Wireless Systems"*, IEEE Journal on Selected Areas in Communications, vol. 21, pp. 281-302.

5. **Bliss D. W., Chan A. M., Chang N. B., (2004),** *"MIMO Wireless Communication Channel Phenomenology"*, IEEE Trans, Antennas Propagation, 52(8), pp. 2073-2082.

6. **Alamouti S. M., (1998),** *"A Simple Transmit Diversity Technique for Wireless Communications"***,** IEEE Journal on Selected Areas in Communications, vol. 16, pp. 1451-1458.

7. **Li X., Chindapol A., Ritcey J. A., (2002),** *"Bit-Interleaved Coded Modulation with Iterative Decoding and 8PSK Signaling"*, IEEE Trans. Communication., vol. 50, pp. 1250-1257.

8. **Li X., Ritcey J. A., (2001),** *"Trellis Coded Modulation with Bit Interleaving and Iterative Decoding"*, IEEE J. Select. Area Communication, submitted for publication, vol. 36, pp. 1004-1012.

9. **Tonello A. M., (2001),** *"Performance of Space-Time Bit Interleaved Codes in Fading Channels with Simplified Iterative Decoding"*, Proc. IEEE VTC, Rhodes, Greece, pp. 1357-1361.

10. **Ungerboeck G., (1982),** *"Channel Coding with Multilevel/Phase Signals"*, IEEE Trans. Inform. Theory, vol. 28, pp. 56-67.

11. **Zehavi E., (1992),** *"8-PSK Trellis Codes for a Rayleigh Fading Channel"*, IEEE Trans. Communication, vol. 40, pp. 873-883.

12. **Jamali S. H., Le-Ngoc T., (1994),** *"Coded-Modulation Techniques for Fading Channels"*, New York: Kluwer, vol. 10, pp. 321-324.

13. **Brannstrom F., Rasmussen L., (2007),** *"Classification of 8PSK Mappings of BICM"*, in Proc. IEEE ISIT '07, pp. 2136-2140.

14. **Lin S., Constello D. Jr., (1982),** *"Error Control Coding: Fundamentals and Applications"*, Englewood Cliffs, Prentice Hall, NJ, pp. 545-547.

15. **Li X., Chindapol A., Ritcey J. A., (2002),** *"Bit-Interleaved Coded Modulation with Iterative Decoding and 8PSK Signaling"*, IEEE Trans. Communication, vol. 50, pp. 1250-1257.

16. **Barbulescu A., Pietrobon S., (1994),** *"Interleaver Design for Turbo Codes"*, IEEE Electronics Letters, pp. 2107-2108.

17. **Khandani A. K., (1999),** *"Optimization of the Interleaver Structure for Turbo Codes"*, Proceeding of the 1999 Canadian workshop on Information theory, pp. 25-28.

18. **Lin S., Constello D. Jr., (1982),** *"Error Control Coding: Fundamentals and Applications"*, Englewood Cliffs, Prentice Hall, NJ, pp. 417-421.

19. **Tan J., Stuber G. L., (2005),** *"Analysis and Design of Symbol Mappers for Iteratively Decoded BICM"*, in IEEE Trans. Wireless Communication, pp. 662-672.

20. **Tran N. H., Nguyen H. N., (2006),** *"Signal Mappings of 8-ary Constellations for Bit Interleaved Coded Modulation with Iterative Decoding"*, IEEE Transactions on Broadcasting, vol. 52, pp. 92-99.

21. **Li X., Ritcey J. A., (1998),** *"Bit-Interleaved Coded Modulation with Iterative Decoding Using Soft Feedback"*, IEEE Electronics Letters, vol. 34, pp. 942-943.

22. **Freng W., Yuan J., Vucetic B., (2002),** *"A Code-Matched Interleaver Design for Turbo Codes"*, IEEE Transactions on Communications, vol. 50, pp. 926-937.

23. **Gertsman M., Lodge J., (1997),** *"Symbol-by-Symbol MAP Demodulation of CPM and PSK Signals on Rayleigh Flat Fading Channels"*, IEEE Transactions on Communications, vol. 45, pp. 788-799.

24. **Berrou C., Glavieux A., (1996),** *"Near Optimum Error Correcting Coding and Decoding: Turbo Codes"*, IEEE Transactions on Communications, vol. 44, pp. 1261-1271.

25. **Sklar B., (1997),** *"Rayleigh Fading Channels in Mobile Digital Communication Systems- Part I: Characterization"*, IEEE Communications Magazine, pp. 90-100.

26. **Sandell M., Luschi C., Strauch P., Yan R., (1998),** *"Iterative Channel Estimation Using Soft Decision Feedback"*, in Proceedings of the Global Telecommunications Conference, Sydney, pp. 3728-3733.

27. **Sklar B., (1988),** *"Digital Communications Fundamentals and Application"*, Prentice-Hall Englewood Cliffs, NJ, pp. 653-655.

28. **Proakis J., Manolakis D., (1992),** *"Digital signal Processing-Principles, Algorithms and Applications"*, Macmillian, pp. 521-524.

29. **Benedetto S., Divsalar D., Montorsi G., Pollara F., (1997),** *"A Soft-Input Soft-Output APP Module for Iterative Decoding of Concatenated Codes"*, IEEE Communications Letters, vol. 1, pp. 22-24.

30. **Hangenauer J., (1988),** *"The Design of Trellis Coded Modulation for MPSK for Fading Channels: Performance Criteria"* IEEE Trans. Communication, vol. 36, pp. 1004-1012.

31. **Benedetto S., Divsalar D., Montorsi G., Pollara F., (1996),** *"A Soft-Input Soft-Output Maximum a-Posteriori (MAP) Module to Decode Parallel and Serial Concatenated Codes"*, TDA Progress Report, pp. 42-70.

32. **Gespert D., (2003),** *"From Theory to Practice: An Overview of MIMO Space-Time Coded Wireless Systems"*, IEEE JSAC, Vol. 21, pp. 580-600.

33. **Tarokh V., Jafarkhani H., Calderbank A. R., (1999),** *"Space-Time Block Coding for Wireless Communications: Performance Results"*, IEEE JSAC, Vol. 17, pp. 307-315.

34. **Liew T. H., Hanzo L., (2002),** *"Space-Time Codes Concatenated Channel Codes for Wireless Communications"*, Proc. IEEE, vol. 90, pp. 187-219.

35. **Divsalar D., Simon M. K., (1988),** *"The Design of Trellis Coded Modulation for MPSK for Fading Channels: Performance Criteria"*, IEEE Trans. Communication, vol. 36, pp. 1004-1012.

36. **Proakis J., (1995),** *"Digital Communications"*, New York, USA: McGraw-Hill: International Editions, 3rd ed. pp. 245-248.

37. **Stoica P., Larson E., (2003),** *"Space-Time Block Coding for Wireless Communication",* Cambridge University Press, pp. 356-359.

38. **Bauch G., (1999),** *"Concatenation of Space-Time Block Codes and Turbo-TCM"*, in Proceedings of IEEE International Conference Communication (Vancouver, Canada), pp. 1202-1206.

39. **Teimouri M., Hedayat A., Shiva M., (2009),** *"Concatenated Bit-Interleaved Coded Modulation and Orthogonal Space-Time Block Codes Over Fading Channels"*, IET Communication, Vol. 3, pp. 1354-1362.

40. **Sklar B., (1997),** *"Rayleigh Fading Channels in Mobile Digital Communication Systems- Part I: Characterization"*, IEEE Communications Magazine, pp. 90-100.

41. **Rappaport T. S., (2002),** *"Wireless Communications: Theory and Practice"*, Prentice-Hall, 2^{nd} Edition, pp. 454.

42. **Clarke R. H., (1968),** "*A Statistical Theory of Mobile Radio Reception"*, Bell Systems Technical Journal 47 (6): pp. 957-965.

43. **William C. J., Editor (1975),** *"Microwave Mobile Communications"*, New York: John Wiley & Sons Inc, pp.180-182.

44. **Smith J. I., (1975),** *"A Computer Generated Multipath Fading Simulation for Mobile Radio"*, IEEE Trans. on Vehicular Technol. Vol. 24, pp. 39-40.

45. **Omidi M. J., Pasupathy S., Gulak P. G., (1999),** "*Joint and Channel Estimation for Rayleigh Fading Channels"*, Wireless Personal Communications Vol. 10: pp. 319-339.

46. **Young D. J., Beaulieu N. C., (2001),** *"Limitations of Sum-of-Sinusoids Fading Channel Simulators"*, IEEE Trans on Communication, Vol. 4: pp. 699-708.

47. **Xiao C., Zheng Y. R., (2002),** *"A Statistical Simulation Model for Mobile Radio Fading Channels"*, Proc. IEEE Wireless Communication and Networking Conf. Vol. 1: pp. 144-149.

48. **Nosratinia A., Hunter T. E., Hedayat A., (2004),** "*Cooperative Communication in Wireless Networks"*, IEEE Communication Magazine, pp. 74-80.

49. **Laneman J. N., Wornell G. W., (2003),** *"Distributed Space-Time Coded Protocols for Exploiting Cooperative Diversity in Wireless Networks"*, IEEE Trans. Inf. Theory, Vol. 49, pp. 2415-2425.

50. **Wornell G. W., Laneman J. N., (2004),** "*Cooperative Diversity in Wireless Networks: Efficient Protocols and Outage Behavior"*, IEEE Trans. Inf. Theory, Vol. 50, pp. 3062-3080.

APPENDICES A

CURRICULUM VITAE

PERSONAL INFORMATION
Surname, Name: Ismaeil, Omar Khaza'al
Date and Place of Birth: 12 May 1978, Mosul
Marital Status: Married
Phone: +90 5318546935
Email: umar_khazal@yahoo.com

EDUCATION

Degree	Institution	Year of Graduation
M.Sc.	Çankaya Univ., Electronic and Communication Engineering	2014
Higher Diploma	University of Technology, Baghdad, Iraq	2002
B.Sc.	University of Mosul, Electrical Engineering Dep., Mosul, Iraq	2001
High School	Al-Mutamezeen Secondary School, Mosul, Iraq	1996

WORK EXPERIENCE

Year	Place	Enrollment
2003- 2012	University of Mosul, Communication Engineering Department, Mosul, Iraq	Instructor
2007-2012	Cisco Networking Academy, Mosul, Iraq	Instructor

FOREIN LANGUAGES
English

PUBLICATIONS

1. **Ismaeil O.**, **GAZİ O.,** 2014, "*Performance of BICM-ID on AWGN and Mobile Communication Channels*," Mühendislik ve Teknoloji Sempozyumu, Çankaya University, Ankara-Turkey.

HOBBIES

Travel, Books, Swimming, Investment